This is the accepted version of the paper: Marin M., **Nikolic M. V**., Vidic J. (2021) Rapid point-of-need detection of bacteria and their toxins in food using gold nanoparticles, Comprehensive Reviews in Food Science and Food Safety **20** 5880-5900 https://doi.org/10.1111/1541-4337.12839

Rapid Point-of-Need Detection of Bacteria and their Toxins in Food using Gold Nanoparticles

Marco Marin[1], Maria Vesna Nikolic[2], Jasmina Vidic[1,*]

[1] Micalis Institute, INRAE, AgroParisTech, Université Paris-Saclay, 78350 Jouy en Josas, France.

[2] Institute for Multidisciplinary Research, University of Belgrade, 11000 Belgrade, Serbia.

***Correspondance** : jasmina.vidic@inrae.fr

Keywords :

Milk; Meat; Foodborne and Waterborne Bacteria; Localized Surface Plasmon Resonance; Biosensing.

ABSTRACT

Biosensors need to meet the rising food industry demand for sensitive, selective, safe and fast food safety quality control. Disposable colorimetric sensors based on gold nanoparticles (AuNPs) and localized surface plasmon resonance are low-cost and easy-to-perform devices intended for rapid point-of-need measurements. Recent studies demonstrate various facile and versatile AuNPs-based analytical platforms for the detection of bacteria and their toxins in milk, meat and other foods. In this review, we introduce the general characteristics and mechanisms of AuNPs calorimetric biosensors, and highlight optimizations needed to strengthen and improve the quality of devices for their application in food matrices.

1. Introduction

Foodborne and waterborne diseases have become a major health issue worldwide, due to their high incidence that is in constant increase over the last 20 years (Law, Ab Mutalib, Chan, & Lee, 2015; Oliver, Jayarao, & Almeida, 2005; Vizzini, Braidot, Vidic, & Manzano, 2019). Foodborne diseases mainly occur through the consumption of foods contaminated with pathogenic bacteria, the most widespread being *Bacillus cereus, Campylobacter jejuni, Salmonella* spp*., Staphylococccus aureus, Listeria monocytogenes, Shigella* spp*., Clostridium botulinum, Clostridium perfringens, Cronobacter sakazakii, Escherichia coli O157:H7, Vibrio* spp*., Yersinia enterocoli* and the Shiga toxin-producing *Escherichia coli*. Additionally, food contaminated with bacterial toxins, including cholera, Staphylococcal enterotoxin B (SEB), Shiga-like toxin, and ricin, represents high health risks as they may cause both acute and chronic foodborne illnesses. Some bacterial toxins, such as SEB or cereulide, are resistant to heat and persist in foodstuffs for long time periods (Ramarao, Tran, Marin, & Vidic, 2020). Foodborne infections cause diseases, when a bacterium establishes itself in the human host after being ingested with contaminated food, or by foodborne intoxication, when the bacterium produces toxins in a food product, which is then ingested by the human host. Symptoms going from light and moderate (diarrhea, stomach ache, vomiting) to severe, such as kidney failure, and even death (Lund, 2015) can occur in the population at risk comprised of immunodepressed or elderly people, newborns and children and also in healthy people exposed to a very high dose of a microorganism.

Food contamination can occur at any stage in the food chain or under improper storage conditions if food safety issues are not taken into account. Meat and meat products, fish and mollusks, eggs and egg products and finally milk and milk products are the most risky foods susceptible to bacterial contamination (Authority, Prevention, & Control, 2018). In 2017, the European Food Safety Authority (EFSA) reported 43,400 illnesses and 4,541 hospitalizations

caused by foodborne outbreaks in Europe (Authority et al., 2018). For the same year, the US Center for Disease Control and Prevention (CDC) reported 841 foodborne outbreaks that led to 14,481 illnesses and 827 hospitalizations across the United State (Dewey-Mattia, Manikonda, Hall, Wise, & Crowe, 2018). These numbers are probably underestimated because many cases are not reported.

The global food industry, valued over US$ 580 billion, concentrates its efforts on preventing food contamination with pathogenic bacteria and food recalls and avoiding huge economic losses. To ensure a safe food supply and to minimize the occurrence of foodborne diseases, it is essential to screen foods for the presence of pathogens. For this, several strategies have been used and improved over the decades. Traditional methods based on bacteria culturing are very sensitive and accurate but time-consuming, expensive, labor intensive and unable to detect bacterial cells in viable but not cultivable (VBNC) status (Deisingh & Thompson, 2002; Nicolo et al., 2011). The possibility to detect and differentiate bacterial strains using molecular methods has emerged by means of the polymerase chain reaction (PCR)-based, and enzyme linked immunosorbent (ELISA) assays. Molecular methods are more rapid than traditional ones, and offer a highly sensitive, selective, and, in some cases, qualitative detection (Vidic et al., 2019). Nevertheless, major drawbacks of molecular methods include the need for trained personnel and sophisticated instrumentation for molecular analysis. They are high-cost and potential overestimation of the target microorganism can occur due to the detection of dead cells. Mass-spectrometry, alone or coupled with MALDI, enables detection of bacterial cells and their toxins with a high specificity and sensitivity (Cao et al., 2020; Domínguez, Frenich, & Romero-González, 2020). However, the lack in portability due to the need for bulky instrumentation, complex chemical procedures and data analysis makes mass-spectrometry unsuitable for point-of-need screening of foods for bacterial contaminations. The emerging miniaturized technologies may offer affordable, user-friendly, rapid

and robust, but also sensitive and specific food safety monitoring at the point-of-need (Choi, Yong, Choi, & Cowie, 2019; Dincer et al., 2019; Vidic et al., 2019).

The need for fast, reliable, sensitive, cost-effective, user-friendly and on-site pathogen detection to ensure food safety and prevent foodborne outbreaks in real-time have pushed the agri-food sector towards nanotechnologies (Swierczewska, Liu, Lee, & Chen, 2012). Biosensors based on gold nanoparticles (AuNPs) have been gaining importance as they enable robust and reliable detection of food contaminants. Due to the Localized Surface Plasmon Resonance (LSPR) phenomenon, AuNPs show tunable color change depending on their size, shape and inter-particle distance (Balbinot, Srivastav, Vidic, Abdulhalim, & Manzano, 2021; Sun et al., 2020; Verma, Rogowski, Jones, & Gu, 2015). Thanks to this peculiarity, AuNPs based assays allow a naked-eye visualization of the results.

In this review, we provide a brief introduction to the detection principles of biosensors based on the phenomenon of localized surface plasmon resonance (LSPR) of gold nanoparticles and subsequently focus on the key parameters (ionic strength, pH, temperature, protein content, recognition elements) that affect the practical application of AuNP plasma sensors in food. The strategies on how to reduce these adverse effects in the detection of bacteria and their toxin in various foods are highlighted, including the application of direct and indirect target mediated aggregation, enzyme mediated detection and lateral flow assays. Finally, a brief outlook on the current challenges and future development of LSPR sensors for food safety is given.

2. Basic concepts and sensor performances

The term “plasmon” was first proposed by Pines and Bohm who described the resonance oscillation of free electrons at the surface of the particle in the presence of light as a surface plasmon resonance (Pines & Bohm, 1952). This phenomenon, also known as a local plasmon

resonance (LSPR), based on the unique optic properties of noble metal nanoparticles, allows the color differentiation of aggregated and non-aggregated particles in a solution. LSPR sensors are commonly based on noble metals (such as gold, silver, platinum, and palladium) because they have an optical absorption band in the visible range of the electromagnetic spectrum. Gold is the most used noble metal in LSPR biosensors because gold can be easily and highly efficiently functionalized with biological molecules, and is compatible with chemically and biologically active molecules. Importantly, AuNPs biosensors can be integrated in various detection platforms (Balbinot et al., 2021; Sun et al., 2020; Zhengguo Wu, Huang, Li, Xiao, & Wang, 2018). Dispersed spherical AuNPs (1 nm-50 nm diameter) in a solution have a wine-red color (plasmonic band is at ~ 520 nm) while aggregated AuNPs have a purple color (plasmonic band is at ~ 630 nm) as illustrated in Fig. 1A. The LSPR phenomenon reflects the collective oscillation of electron gas of AuNPs due to the interaction of free surface electrons with light. The charge polarization on the NPs surface establishes a dipolar field, which in turn, impacts the absorption and scattering of light, as illustrated in Fig. 1B (Chang et al., 2019; Motl, Smith, DeSantis, & Skrabalak, 2014). The plasmon oscillation and the consequent color of AuNPs in a solution (dielectric medium) is highly affected by the inter-particle distance: the more the distance between AuNPs is reduced, the intensity of the change in color from red to purple is greater. AuNPs are also commonly used together with Raman spectroscopy for Surface Enhanced Raman spectroscopy (SERS) analysis. Raman and SERS analysis with AuNPs has shown the capability to analyze various food contaminants, such as toxins, pesticides, and microorganisms. Some recent reviews have addressed the use of AuNPs for analysis in foods when coupled to Raman spectroscopy (Balbinot et al., 2021; Lin & He, 2019).

The simplest and most commonly used method to synthesize gold nanoparticles is the citrate reduction method. First reports on AuNP synthesis by reduction of gold (III) salt (usually $HAuCl_4$) by trisodium citrate go back to the 1940s (Hauser & Lynn, 1940). The citrate reduction

method was developed by Turkievich et al., in 1951 (Turkevich, Stevenson, & Hillier, 1951), and further optimized by Frens (Frens, 1973) to enable control of the nanoparticle size by varying the trisodium citrate content. The role of sodium citrate is twofold: it functions as a weak reducing agent and a capping agent stabilizing nanoparticles. The ratio between the gold salt and citrate controls the particle size (Dong, Carpinone, Pyrgiotakis, Demokritou, & Moudgil, 2020; Pong et al., 2007). Besides trisodium citrate, other reductants have been used, such as sodium borohydride (Jana, Gearheart, & Murphy, 2001), tannic acid (Slot & Geuze, 1984), ascorbic acid (Kimling et al., 2006), amine molecules (Niidome, Nakashima, Takahashi, & Niidome, 2004) or dextran (Y. Wang, Zhan, & Huang, 2010). Modifications of the synthesis protocol have resulted in AuNPs with different geometrical shapes as a result of controlling the pH and precursor to reductant concentration and room temperature synthesis (Tyagi, Kushwaha, Kumar, & Aslam, 2016). One modification is the “seed-mediated growth method” as initially formed small AuNP seeds grown in solution are used to synthesize AnNPs with controlled morphology and dimensions (Bastús, Comenge, & Puntes, 2011). Systematic small manipulation of synthesis parameters can result in varied shapes and sizes of AuNPs in aqueous solution at room temperature (Sau & Murphy, 2004).

To control the aggregation state of AuNPs for detection purposes, it is essential to manage their stability in the solution. The aggregation state of AuNPs depends on the equilibrium between the electrostatic repulsive force and van der Waals attractive force in a solution containing nanoparticles, recognition elements and the target. Two main strategies, electrostatic and steric, are used to stabilize AuNPs. Electrostatic stabilization is achieved by the addition of molecules with a similar electrical charge as ions in the medium, in order to form a repulsive electric double layer and disperse AuNPs. Steric stabilization is obtained upon binding of ligands to the NPs to create a physical hindrance to particle aggregation (Aldewachi et al., 2018). To enable detection of

a target, its addition to the solution has to alter the AuNPs aggregation state and consequently change the solution color as illustrated in Fig. 1C.

The target may induce AuNPs aggregation by cross-linking or by a simple adsorption/desorption process (Zhengguo Wu et al., 2018). Upon cross-linking, specific bonds are created among aggregated AuNPs while in non-cross-linking the interaction occurs between the recognition element and a biomarker (Aldewachi et al., 2018). In the second case, the ionic strength of the solution controls the aggregation of AuNPs. Detection methods based on interparticle crosslinking aggregation of AuNPs were first developed by Mirkin and co-workers (Elghanian, Storhoff, Mucic, Letsinger, & Mirkin, 1997; Giljohann et al., 2020; Mirkin, Letsinger, Mucic, & Storhoff, 1996).

The most common recognition elements are ssDNA probes, antibodies, peptides, bacteriophages and aptamers. DNA probes detect specific nucleic acid sequences of a pathogen. Storhoff et al., established that the aggregate size is crucial for optical properties of DNA-linked nanoparticle assemblies (Storhoff et al., 2000). Prasad et al, have developed a colorimetric genosensor for naked-eye detection of *Salmonella* spp. in food samples (Prasad & Vidyarthi, 2011). The biosensor detected PCR products using a complementary ssDNA probe immobilized onto AuNPs. Before addition of PCR products, the probe was adsorbed on colloidal gold nanoparticles and prevented their aggregation. Upon probe hybridization with the target DNA, the formed dsDNA desorbed from AuNPs inducing color change of the solution from red to purple. The sensitivity of this colorimetric assay was higher than gel based visualization of the same PCR products.

Antibodies, peptides, bacteriophages and aptamers can target whole bacterial cells. Employment of such recognition elements drastically simplifies the test, by shortening sample

preparation prior to analysis, which significantly reduces the time and the cost of the assay. For instance, thiolated chimeric phages displaying different specific receptor binding proteins that naturally target the desired bacterial species were incubated with bacteria, including *Pseudomonas aeruginosa*, *Escherichia coli*, and *Vibrio cholera* and added to AuNPs colloidal solution. The covalent attachment of phages-bacteria complexes to AuNPs, due to the formation of thiol-gold bonds, induced aggregation of AuNPs and generated a colorimetric signal (Peng & Chen, 2018). This strategy demonstrated rapid and specific bacterial detection, with a limit of detection (LoD) of ~ 100 cells.

3. Critical parameters

The LSPR phenomenon reflects the size, composition, morphology, inter-particle distances, and orientation of plasmonic nanostructures. Performances of a LSPR colorimetric test in food matrices may be compromised by food components that alter these parameters. Ascorbic acid, ions, such as Cl^-, Ca^{2+}, Na^+, K^+, SO_4^{-2} and PO_4^{3-}, carbohydrates such as dextrose or sucrose, proteins and amino acids are all reported to interfere with the detection process (Paul et al., 2017). This is particularly the case in assays using non-modified AuNPs that are highly sensitive to the surrounding medium. The dynamics of physico-chemical interactions between food matrix components and AuNPs has to be analyzed and predicted in order to design signal transducers for a visual readout.

The buffer plays a crucial role in LSPR colorimetric detection. The ionic strength of the buffer may modify the adsorption capacity of AuNPs and their aggregation state (X. Zhang, Servos, & Liu, 2012). Water soluble salts, such as $MgSO_4$, NaCl or $MgCl_2$, are usually used to adjust the ionic strength of the buffer and optimize the sensors' analytical parameters (H.-S. Kim et al., 2017; Y.-J. Kim et al., 2018; Ledlod, Areekit, Santiwatanakul, & Chansiri, 2020). Salts neutralize the repulsive forces between gold nanoparticles, which perturbs the equilibrium between Van Der

Waals attractive and electrostatic repulsive forces, and favors particle aggregation (Gao, Huang, Liu, Zan, & Ren, 2012; Ledlod et al., 2020). A higher ionic straight results in faster aggregation and lower sensitivity (Hianik, Ostatná, Sonlajtnerova, & Grman, 2007). For instance, Hianik et al. showed a decrease of the sensor sensitivity with the increase of salt concentrations (Hianik et al., 2007). Interestingly, Su et al. showed that the interferences of various common ions were not the same in the colorimetric test for *E. coli* O157:H7 detection (Su et al., 2012). No color change was observed upon addition 1 mM Al^{3+}, Mg^{2+}, K^{+}, Cl^{-}, SO_4, and NO_3, but the addition of 0.1 mM Ca^{2+} resulted in a color change. This indicated that Ca^{2+} from a food sample could bring out false positive results for bacterial detection using the assay.

The pH of the solution is another critical factor because the pH influences the surface charge of AuNPs, and electrostatic interactions involved in binding processes (Su et al., 2012; A. Wang, Perera, Davidson, & Fitzkee, 2016). Jiang et al. reported faster binding of non-thiolated DNA onto negatively charged AuNPs at pH 3 than at the neutral pH (Jiang, Materon, Sotomayor, & Liu, 2013). Similarly, Ma et al. showed that adsorption of DNA onto AuNPs at pH 3 required only a few minutes, while at neutral pH several days were needed (Requena, Vargas, & Chiralt, 2018), and Zhang et al. highlighted the decrease in adsorption of DNA at AuNPs for increasing pH (X. Zhang, Liu, Servos, & Liu, 2013). The facilitation of DNA adsorption onto AuNPs at acidic pHs originates probably from the protonation of adenine and cytosine and reduction of the DNA negative charge. However, pH 3 was not found to be an optimal pH in the majority of publications. For instance, Kim et al. determined pH 5.5 as the most suitable pH since it promoted DNA adsorption and improved stability of conjugates, while other authors asserted a pH range from neutral to slightly basic (pH 7.3 - 8.2) as the most suitable due to the stabile equilibrium between attractive and repulsive forces at the surface of AuNPs (Hianik et al., 2007; Ledlod et al., 2020). It appears, thus, that the most suitable pH of the solution cannot be standardized but should be optimized for each

test and each food matrix. In addition, some variations of pH may denature proteins and oligonucleotides and block the recognition event.

The influence of the assay temperature on sensitivity was likewise stressed. The adsorption rate of a biomolecule onto AuNPs depends on the temperature (H. Li & L. J. Rothberg, 2004; Vial, Nykypanchuk, Deepak, Prado, & Gang, 2014). Ideally, a binding rate of about 50 % is achieved when a short oligonucleotide (< 40 nucleic acid bases) is incubated with AuNPs at 37°C for 30h (Requena et al., 2018). However, the binding rate becomes lower upon temperature decrease, which may disable the point-of-care detection of pathogens at room or refrigerated temperatures applied for food storage. Feng et al. observed that the binding rate of about 40 % was reached upon incubation of an aptamer with AuNPs at 37°C for 24h, while the binding rate decreased to 32% and 20% at 15°C and 4°C, respectively (Feng, Shen, Wu, Dai, & Wang, 2019). On top of that, it is better to perform assays at higher temperatures when possible. The downside risk in excessive temperature increase is a secondary structure modification of biomolecules, and loss in sensor sensitivity (H. Li & L. J. Rothberg, 2004).

The interactions between DNA and AuNPs have been extensively studied because the majority of LSPR colorimetric assays use the DNA detection probe. Although both ssDNA and dsDNA are negatively charged molecules, ssDNA adsorb faster than dsDNA onto AuNPs. Single and double DNA strains have different electrostatic properties in their native conformation due to the different exposition of negatively charge phosphate backbones to the solution (Bloomfield & Crothers, 2000). The uncoil-capacity of ssDNA enables a higher exposition of its bases and facilitates adsorption, while the double helix of dsDNA presents negatively charged backbones to the negatively charged AuNPs (Y. S. Kim, Kim, Kim, Lee, & Gu, 2011; F. Li et al., 2018; H. Li & L. Rothberg, 2004). The adsorption rate also depends on the sequence length, with short oligonucleotides (< 40 nucleic acid bases) binding more rapidly to AuNPs (H. Li & L. J. Rothberg,

2004; X. Zhang et al., 2012). Short sequences are more stably adsorbed on AuNPs and protect them better from aggregation than long ones (F. Li et al., 2018; Y. Luo et al., 2015). Additionally, the adsorption rate is base-discriminative, thus adenine has the highest affinity to Au surfaces, followed by cytosine, guanine and thymine (Jiang et al., 2013; H.-S. Kim et al., 2017). The sensor stability can be increased by adding a short adenine base linker at one end of the DNA sequence (Y.-J. Kim et al., 2018; X. Zhang et al., 2013). Finally, to optimize analytical performances of a LSPR sensor it is necessary to adjust the DNA/AuNP concentration ratio as demonstrated in many publications (Q. Fang et al., 2019; H.-S. Kim et al., 2017; Y.-J. Kim et al., 2018; Y. S. Kim et al., 2010; Y. Luo et al., 2015; Ma, Song, Zhou, Xia, & Wang, 2017; Requena et al., 2018; Yuan et al., 2014).

Oligonucleotides are commonly tagged with the thiol group at one end to enable their covalent binding to AuNPs via S-Au bonds to improve the stability of DNA/AuNPs complexes. The high stability of these complexes offers improved resistance to salts and other molecules from food matrices, thermal treatment or pH variations (Gao et al., 2012; Zhengguo Wu et al., 2018).

4. Protein adsorption on AuNPs

Proteins, as essential molecules, are present in almost any type of food. They interact readily with Au NPs and form a corona shell around particles. Its thickness and structure depends on the medium composition but also on the NPs' physicochemical properties and time of exposure (García-Álvarez, Hadjidemetriou, Sánchez-Iglesias, Liz-Marzán, & Kostarelos, 2018; Piella, Bastús, & Puntes, 2017). Wang et al., have shown that a protein corona created by albumin adsorption on Au NPs decreased the detection signal of the LSPR sensor by more than 20% compared to the detection signal observed in a buffer solution containing no protein (H. Wang, Dardir, Lee, & Fabris, 2019). Most research on protein corona formed around AuNPs has been performed using biological fluids or cell media with only a very few dealing with this point using food matrices.

Recently, Tao et al., selected milk as a model and showed that milk protein corona disturbed AuNP-aptasensors, AuNP-immunosensors and AuNP-dichlorofluorescent sensors decreasing their sensitivity up to 80% (Tao et al., 2020). In addition, the polyethylene glycol backfilling strategy was ineffective in mitigating the protein corona negative effect. This demonstrates that AuNPs-based sensors should be calibrated in each food matrix to provide the test accuracy.

4.1. Indirect target mediated AuNPs aggregation

In direct LSPR assays, AuNPs aggregation is triggered by the stronger interaction between the stabilizer (aptamer, antibody) and target causing detachment of the stabilizer from the gold nanoparticle surface resulting in a color change, as illustrated in Fig. 2A. Most label-free LSPR sensors function as direct assays. However, many molecules, especially proteins, present in food samples could additionally stabilize AuNPs and lead to detection failure by preventing AuNPs aggregation. Indirect target mediated AuNPs aggregation, as a two-step procedure has been proposed to minimize potential interference from the matrix factors (Fig. 2B). In the first step, aptamers/antibodies are mixed into the sample to allow their binding to the target bacterium. Then, aptamers/antibodies can be easily depleted from the solution using centrifugation. Using a supernatant in the second stage enables AuNPs to aggregate, resulting in a color change. In the absence of target bacteria, target-specific sensing elements cannot be removed by centrifugation in the first step. Freely diffused aptamer/antibodies in the supernatant adsorb onto AuNPs in the second step and prevent salt-induced aggregation and solution color change. Indirect target mediated tests have been successfully applied to bacterial detection in powdered infant formula (H.-S. Kim et al., 2017) and chicken meat (Y.-J. Kim et al., 2018).

4.2. Enzyme mediated detection

Sensitivity and specificity of LSPR assays can be improved by coupling AuNPs to an enzymatic reaction. Wu et al. have developed a colorimetric aptasensor for the detection of *Vibrio parahaemolyticus* cells (S. Wu, Wang, Duan, Ma, & Wang, 2015). The aggregation of AuNPs occurred in the presence of *V. parahaemolyticus* due to a sandwich complex formation. Two different aptamers targeting bacterial whole cells were used: the first, Apt1, was thiolated and covalently linked to AuNPs via gold-thiol conjugation, while the second, Apt2, was biotinylated and attached by affinity to the avidin-modified magnetic nanoparticles (MNPs), as shown in Fig. 3. In addition, horseradish peroxidase (HRP) was immobilized onto AuNPs-Apt1. After incubation of *V. parahaemolyticus* with AuNPs-HRP-Apt1 and MNPs-Apt2 in a solution, a magnetic field was applied to collect the AuNPs-HRP-Apt1-Target-Apt2-MNPs complexes. Subsequently, addition of the HRP substrate, tetramethylbenzidine (TMB), in the presence of H_2O_2, generated a colorimetric signal proportional to the bacteria concentration. A LoD as low as 10 CFU/mL was reached. In the absence of targeted bacterial cells, free AuNPs-HRP-Apt1 were not collected by the magnet and no signal was observed upon TMB addition.

Bacterial toxins can be detected using their cleaving enzyme as recognition elements. For instance, a rapid and sensitive colorimetric assay for botulinum neurotoxins serotype A light chain (BoLcA), produced by *Clostridium botulinum*, was developed by Liu et al. (X. Liu et al., 2014). Two specific peptides cleaved by BoLcA were used: Peptide1 carrying a biotin tag at one terminus and a thiol tag at the other, and bi-biotinylated Peptide2. In the first strategy, Peptide1-AuNPs aggregated upon the addition of neutravidin-functionalized AuNPs due to particle cross-linking. In the presence of BoLcA, Peptide1 was cleaved and no aggregating occurred. The LoD of this essay was 5 nM of BoLcA. In the second strategy, Peptide2 with two biotin moieties, one at each terminus was used to bridge neutravidin-AuNPs. Again, cleavage of the peptide prevented

nanoparticle aggregation. The LoD obtained with the second strategy was only 0.1 nM of BoLcA. Utilization of enzymes attached to gold nanoparticles allows applications in various matrices. However, molecules such as proteins, or fats and ions from some foods may inhibit enzymatic reactions.

Some examples of AuNPs -based biosensors for bacteria and their toxin detection are given in Table 1.

4.3. Lateral flow

Colorimetric methods may be performed on a flat substrate format enabling separation of some proteins from the target. Lateral flow assays performed on paper substrates, which use AuNPs as a color marker, are probably the most used point-of-need tests covering a variety of applications. In lateral flow assays, the sample is guided through capillary movement over different functional membranes (Sajid, Kawde, & Daud, 2015). As illustrated in Fig. 4, a standard lateral flow strip has four main parts: sample pad, made of cellulose, where the sample is dropped; conjugate pad, made of glass fiber, containing AuNPs bioconjugated with the first recognition element (antibody, aptamer); detection pad, a nitrocellulose sheet where the result is reveled on the test line (TL), containing a second recognition element for the target, and the control line (CL) containing a probe that binds to the first recognition element; and finally the absorption pad made of cellulose. The capillary movement provides target separation from surrounding proteins and other materials from the sample matrix (Quesada-González & Merkoçi, 2015). To improve the separation, additional filters can be integrated on the sample pad preventing migration of large particles. However, filters cannot be employed when whole bacterial cells are targeted. Alternatively, the sample pad may contain pre-stored reagents to stabilize pH and ionic strength in order to increase specific and decrease non-specific binding to AuNPs. Then, the solution flows from the sample pad

to the conjugate pad, where the bioconjugated AuNPs recognize the target in the first recognition event. The solution then continues to flow along the detection pad, where the complex target/labelled-antibody(aptamer) binds to the capture element of the TL, during the second recognition event. Finally, the sample passes through the CL and arrives to the absorbent pad. The sensitivity of a lateral flow assay maybe improved by decreasing the flow-rate and increasing the time of the test by engineering the pad structure (Sena-Torralba et al., 2020; S.-F. Zhang et al., 2019), by optimizing the concentration of recognition element on the surface of AuNPs (Byzova, Safenkova, Slutskaya, Zherdev, & Dzantiev, 2017), or by increasing the amount of the capturing antibody on the TL (Pan et al., 2018).

Despite the many advantages of colorimetric methods performed on flat substrate format over those performed in solution there are still some technical drawbacks especially for samples containing high concentrations of proteins. A protein corona formed over AuNs may prevent the binding event and the test may give a false negative result, or the corona composition may non-specifically bind to some particles in the sample and provide a false positive result. False positive results may be remove by adding sucrose, tween or by nitrocellulose pretreatment (de Puig, Bosch, Carré-Camps, & Hamad-Schifferli, 2017).

5. Bacterial cells and toxin detection in milk

Milk is one of the most challenging food matrices for bacteria and toxin detection using colorimetric sensors. Milk is a colloidal solution composed of water, butterfat globules, carbohydrates, protein complexes and various minerals (Quigley et al., 2013). It can support the growth of diverse microorganisms, because in addition to being highly nutritious, milk is of near neutral pH and has a high water activity. Due to bacterial ubiquitous presence in air, soil, water,

and dairy plant environments, milk can be contaminated by pathogenic bacteria not only in farms but also during processing, storage and distribution (Vidic, Chaix, Manzano, & Heyndrickx, 2020). Thermoduric bacterial strains, such as *Bacillus cereus*, sulphate-reducing clostridia, *Salmonella* spp., *Listeria* spp., coagulase-positive staphylococci, *Escherichia coli*, and *Enterobacteriaceae* survive pasteurization, while psychotropic bacterial strains such as *Pseudomonas* and *Acinetobacter* spp. are frequently established in milk during cold storage (Quigley et al., 2013). Besides that, *Staphylococcus aureus*, *Escherichia coli* O157:H7, *Cronobacter sakazakii* and *Campylobacter* are pathogens that contaminate milk if hygienic milking conditions are not fully respected.

Among milk ingredients fat, lipids, Ca^{2+}-ions, and proteins are potent inhibitors of the LSPR phenomenon and may interfere in bacterial detection. Several strategies for milk treatment prior to analysis have been proposed in order to eliminate these inhibitory components from milk. For instance, fats can be easily scooped out from milk after sample centrifugation because they rest floating (Marathe, Chowdhury, Bhattacharya, Nagarajan, & Chakravortty, 2012). Proteins, such as casein and whey, precipitate upon addition of 0.5 M EDTA (Marathe et al., 2012). Similarly, proteins can be precipitated by decreasing the pH of skimmed milk (Haddada et al., 2017). A mixture of trichloroacetic acid and chloroform was shown to dissolve fats and other organic molecules and deposit proteins in a one minute procedure (Y. Luo et al., 2015). Otherwise, subsequent 1 min vortexing of milk samples after addition of potassium hexacyanoferrate (II) tryhydrate and zinc sulfate efficiently precipitate proteins and fats (Kumar, Seth, & Kumar, 2014). Such procedures involve centrifugation steps to separate bacterial fractions from the assay inhibitors. *Cronobacter sakazakii* was successfully detected in milk and infant formula using an enhanced lateral flow assay but samples were centrifuged and re-suspended to remove lipids and proteins before being deposited on the sample pad (Pan et al., 2018). Such sample pretreatment

limits point-of-need applications of the test. Using this strategy, the sensitivity of the enhanced lateral flow for detection of *C. sakazakii* in powdered infant formula was 10^3 CFU/mL and the time of analysis was 3 h. Traditional microbiological methods take 5 to 7 days to complete analysis of *C. sakazakii* and cannot be performed on-site.

In some cases, centrifugation steps can be replaced by portable separation methods like filtration (Requena et al., 2018), or magnetic separation (Cho & Irudayaraj, 2013; Duan, Xu, Wu, & Wang, 2016; Kotsiri et al., 2019; Poshtiban et al., 2013; Quintela, de los Reyes, Lin, & Wu, 2019). For instance, Duan et al. applied magnetic nanoparticles (MNPs) as bacterial concentration elements and aptamer AuNPs as colorimetric probes for detection of *S. thyphimurium* in spiked milk (Duan et al., 2016). Two specific aptamers were employed, Apt1 modified with a thiol group (Apt1) was stability immobilized onto AuNPs and Apt2 modified with biotin was specifically bound to streptavidin coated MNPs. In the presence of *S. thyphimurium*, gold nanoparticles aggregated upon formation of MNPs-Apt2-*S.typhimurium*-Apt1-AuNPs complexes that were collected by an external magnet. Aggregation induced fading of the solution red color visible to the naked eye. The assay enabled a quantitative detection of *S. thyphimurium* because the peak intensity at 520 nm was proportional to the bacteria concentration. The limit of detection of only 10 CFU/mL was reached in milk. The sensitivity of standard molecular methods for detection of *S. thyphimurium* was found to be around 10^3 CFU/mL in milk and meat samples (Perelle et al., 2004).

Kim et al. developed a two-stage label-free aptasensor for detection *Cronobacter sakazakii* in powdered infant formula (H.-S. Kim et al., 2017). First, the bacteria was incubated with the aptamer for a few minutes. Then the solution was centrifuged to precipitate bacterial-aptamer complexes and milk proteins. AuNPs were added to the supernatant, and their aggregation was induced with NaCl (Fig. 3a). This aggregation and the color change of the solution were dependent on the *C. sakazakii* concentration: more bacterial cells in the sample resulted in less aptamer

molecules remaining in the supernatant. The color change from red to purple was the most pronounced in supernatants without aptamers because their adsorption onto AuNPs prevented nanoparticle aggregation after NaCl addition. The LoD of 7.1 x 10^3 CFU/mL was reached in the spiked infant formula with a total detection time of 30 minutes.

A sensitive colorimetric test for the detection of *Campylobacter jejuni* in milk was developed exploring aptamer binding to Au coated palladium nanoparticles (Au@PdNPs) (Dehghani, Hosseini, Mohammadnejad, Bakhshi, & Rezayan, 2018). In this case AuNPs were synthesized using a modified Turkievich method, resulting in AuNPs of 50 and 58 nm. Au@PdNPs exhibited an enzyme-like activity. As depicted in Fig. 3b, after sample incubation with a specific ssDNA aptamer followed by centrifugation, Au@PdNPs were added to the supernatant containing the unbound aptamers. The peroxidase activity of Au@PdNPs for 3,3”,5,5”-tetramethylbenzidine (TMB) oxidation was used as a reporter to evaluate the concentration of *C. jejuni* in samples. Following an enzymatic reaction instead of AuNPs aggregation, makes the test less sensitive to the presence of milk proteins and fats and, thus, simplifies sample preparation. In the aptamer-free supernatant, showing evidence of the presence of target bacteria, the oxidative reaction of TMB by H_2O_2 occurred and the color turned from transparent to blue. On the contrary, in the presence of aptamers, in the absence of target bacteria, the oxidative reaction could not occur because aptamer binding to NPs inhibited their activity. Different concentrations of *C. jejuni* led to a different blue color shade as shown in Fig. 3c. The LoD of the sensor was 100 CFU/mL. This aptasensor shows advantage over molecular methods, such as PCR-based methods, that may provide false-negative responses because of the sensitivity of DNA polymerase to inhibitors present in food matrices and enrichment broths (Vizzini et al., 2019).

Recently, a portable, and label-free gold nanodisk-based LSPR sensing chip was reported for sensitive detection of *S. aureus* in milk (Khateb, Klös, Meyer, & Sutherland, 2020). The sensor performance was optimized through different designs specifically addressing the role of the near-field and intrinsic refractive index sensitivity. By tuning the detection readout from optical to the near-infrared, a good sensor performance was obtained employing aptamers as recognition elements. The LoD of 10^3 CFU/mL was obtained for *S. aureus* in artificially contaminated milk samples without a pre-enrichment step in less than 5 min. However, when the aptamer was replaced by an anti-*S. aureus* antibody a decrease in sensitivity was observed indicating the thickness of the sensing layer as a critical parameter.

Staphylococcal enterotoxin A (SEA) was quantitatively detected in milk using AuNPs based LSPR immunosensors (Haddada et al., 2017). The citrate/tannic acid reduction method adapted from (Slot & Geuze, 1984) was used to synthesize AuNPs with an average size of 13.5 nm. Specific anti-SEA antibodies were treated by Traut's reagent to convert some of their primary amino groups to thiol groups to enable conjugatation with AuNPs. In the direct washing-free detection, SEA was added to the solution containing AuNPs-antibody conjugates and color changes were monitored in real-time. SEA binding to the anti-SEA antibodies attached to AuNPs changed the local refractive index in NPs vicinity and turned the color of the solution from red to purple. The LoD of SEA was estimated to be 5 ng/mL suggesting that such a nanoplasmonic immunosensor is an attractive alternative to more bulky and expensive classical approaches for detection of SEA.

The detection sensitivity can be enhanced by coupling an enzymatic reaction to functionalized AuNPs. For instance, HRP-labeled immuno-gold particles were used for *in-situ* detection of *E. coli* O157:H7, *S. enteritidis*, *L. monocytogenes* and *S. typhimurium* in reduced-fat milk (Cho & Irudayaraj, 2013). Gold nanoparticles on average 30 nm in diameter were synthesized using the citrate reduction method (Pong et al., 2007) and coupled with two types of antibodies.

The immuno-magnetic separation using MNPs decorated with the bacterium-specific antibody1 was first performed to separate and concentrate the bacterial cells from milk. When AuNPs functionalized with the antibody2 that recognized and bound to a complementary bacterial surface epitope were added to the solution, AuNPs-antibody2-bacterium-antibody1-MNPs complexes were formed. To enable highly sensitive detection AuNPs carrying HRP-labeled secondary antibodies that bind to antibody1 and 2, were added to form a network structure that grew with time. The colorimetric signal produced upon addition of TMB and H_2O_2 enabled detection of different bacteria in milk with the LoD of 3-15 CFU/mL within only 2 h.

Another strategy to increase the sensitivity of bacterial detection in food consists in coupling LSPR with a PCR amplification (S. Chen et al., 2020; R. Luo et al., 2014; Prasad & Vidyarthi, 2011). For instance, Chen et al. specifically detected *S. typhimurium* in spiked milk samples using two different aptamer probes, Apt1 and Apt2 (S. Chen et al., 2020). After a specific enriching of *S. typhimurium* using MNPs-Apt1, Apt2 was added to create MNP-Apt1- *S. typhimurium*-Apt2 sandwiches as shown in Fig. 5. Then, magnetic beads were collected, and heated to liberate Apt2, which was used as a PCR template. Generated PCR products hybridized with their complementary oligonucleotides attached to AuNPs and strongly prevented nanoparticle aggregation upon salt addition. In contrast, no PCR products were formed in the case of non-contaminated samples, and AuNPs aggregated. Due to the production of a large amount of PCR products this assay enabled a naked eye read out with a detection limit of 95 CFU/mL *S. typhimurium* in spiked milk.

Recent results employing AuNPs-based detection strategies to detect bacteria and their toxins in milk are given in Table 1. AuNPs applied in these tests were generally in the range 10-50 nm, either purchased (Sung et al., 2013) or obtained using different modifications of the citrate reduction method (Haddada et al., 2017; Kumar et al., 2014) including seed growth (M. Chen et al., 2015; Hwang, Kwon, Lee, & Jeon, 2016; H. b. Liu et al., 2019; Peng, Borg, Nguyen, & Chen, 2020)

and the modifications introduced by Grabar et al., (Grabar, Freeman, Hommer, & Natan, 1995). The seed mediated gold nanoparticle growth procedure of Bastus et al., (Bastús et al., 2011) was employed by (Peng et al., 2020) to synthesize 7, 20, 50 and 85 nm AuNPs. The smallest NPs were used as seeds for growth of larger NPs. The effect of AuNP size and colloidal stabilization was investigated, and showed that the assay remained stable to different sample media, but change in AuNP size and surface coating significantly influenced the sensitivity. Larger NPs that were citrate coated were overly stable rendering a stable colloid that resulted in no NP aggregation. PEG coating of all sized AuNPs also resulted in high stability and inactive bacteria detection.

6. Bacterial cells and toxin detection in meat

Meat is rich in proteins, poor in carbohydrates and contains many micronutrients such as iron, selenium, vitamins A, B12 and folic acid. Meat structure is very complex containing repetitive myofibrillar protein systems with a high content of active water. Although important biotechnological advancements have been made to improve meat safety, meat-based foods are still under survey because of their contamination by pathogens, causing outbreaks and economic losses. Indeed, meat has to be kept safe in sanitation at every step, starting from the farm. Fresh meat has to be controlled for *Salmonella (*pork, poultry and turkey meat)*, Campylobacter* (broiler meat)*,* enterohaemorrhagic *E. coli* including serotype O157:H7 (meat from ruminants), and other enteric pathogens (Sofos, 2008).

To counteract the persistent foodborne outbreaks caused by ingestion of contaminated meat, rapid colorimetric assays that can be performed at any step of meat production could help the industry improve production management, reduce overheads and prevent public health concerns. Kim et al. developed a LSPR test for *C. jejuni* and *C. coli* in a

chicken carcass rinse with a sensitivity and specificity comparable to the culture method (Y.-J. Kim et al., 2018). A specific aptamer for live *Campylobacter* cells was truncated and tagged with adenine to minimize the incubation time with AuNPs to only 20 min. A two-stage procedure comprised of incubation of the aptamer and bacteria, and addition of AuNPs to the supernatant containing the unbound aptamers. The solution color varied from red to purple in tune with the aptamer and bacterial concentration ratios. The overall analysis was performed within 30 minutes but required a 48h enrichment step. However, the aptamer was shown to bind only spiral *Campylobacter* cells. This limits the sensor application for on-site chicken carcass screening because *Campylobacter* may change its cell shape from a spiral to a coccoid under unfavorable conditions like during cold storage (Duqué, Haddad, Rossero, Membré, & Guillou, 2019; Vizzini et al., 2019). However, the official ISO 10272–1:2006 and ISO 10272-1:2017 methods for *Campylobacter* detection may also provide false negative results because *Campylobacter* may die during handling or enter in a viable but not cultivable (VBNC) status in food matrices, making their detection based on culturing impossible (Vizzini et al., 2020).

A highly sensitive and selective portable LSPR sensing chip was developed for detection of *S. typhimurium* in pork meat samples without a pre-enrichment step (Oh et al., 2017). Prior to functionalization with specific aptamers, AuNPs were self-assembled into a 20 nm monolayer on glass slides. This high-density deposition on a transparent substrate produced longitudinal wavelength extinction shifts via a LSPR phenomenon upon target binding. The LoD was of about 10^4 cfu/mL for *S. typhimurium* in the spiked pork meat samples with a total test time of 30–35 min. Moreover, the developed LSPR sensing chips were not susceptible to components of the food matrix or background contaminant microflora.

Wachiralurpan et al. developed a LAMP-LSPR assay for detecting *L. monocitogenes* in raw chicken meat samples (Wachiralurpan et al., 2018). After DNA extraction and isothermal amplification of the *plcB* gene of *L. monocitogenes*, the LAMP products were directly mixed with AuNPs carrying the complementary DNA probe. A thiolated probe was used to increase the robustness of the test. As illustrated in Fig. 6a, after salt addition, the solution color changed from red to purple in the absence of LAMP products, but remained red when polymeric DNA networking was formed on AuNPs upon hybridization preventing AuNPs aggregation. The LoD of 2.82 CFU/mL was calculated for this test that took only 10 minutes for hybridization, which can be performed using only a heater block. An additional 1 min was needed for the observation of results. This suggested the possibility of user-friendly on-site sensor applications for chicken meat screening.

An UV-Vis spectroscopic measurement of the solution color changing from red to purple can be replaced by smart phone imaging for quantitative on-site bacterial detection. Recently, Zheng et al. developed a microfluidic biosensor based on AuNPs aggregation and smart phone imaging for simple, rapid and sensitive detection of *E. coli* O157:H7 in chicken meat (Zheng et al., 2019). The detection sensitivity was increased using a HRP/H_2O_2/tyramine read out. Bacterial cells were concentrated by MNPs carrying the capture antibodies against *E. coli* O157:H7 and polystyrene microspheres functionalized with detection antibodies directed against *E. coli* O157:H7 (Fig. 6b). In the first mixing channel of the microfluidic chip, *E. coli* O157:H7 cells were mixed with the catalases and functionalized MNPs. The MNP-bacteria-PS complexes were then captured and separated in another chamber by an external magnetic field. Then, H_2O_2 was injected and catalyzed by the catalases on the complexes. The obtained catalysate was mixed with the AuNPs and the crosslinking agent tyramine in the second mixing channel and incubated in the detection chamber. Aggregation of AuNPs was triggered

through the crosslinking of phenolic hydroxyl moieties in tyramine which resulted in the color changing from blue to red. The color was imaged and analyzed by an imaging application on an Android smart phone. This automatized assay exhibited a good specificity and sensitivity for detection of *E. coli* O157:H7 in chicken samples with a LoD of 50 CFU/mL. Some existing methods for detection of *E. coli* O157:H7, such as culture plating or PCR-based methods, have high reliability and sensitivity, but all are time-consuming and generally need 2–3 days to provide results.

Recent results employing AuNPs-based detection strategies to detect bacteria and their toxins in meat are given in Table 2. AuNPs for detection of bacteria and toxins in meat were either purchased choosing an average size of 15-20 nm (Y.-J. Kim et al., 2018; Wachiralurpan et al., 2018), or synthesized using the citrate reduction method with an average size of 15 - 30 nm (Cho & Irudayaraj, 2013; Ledlod et al., 2020; H. b. Liu et al., 2019). Bu et al., (Bu et al., 2019) synthesized two types of AuNPs: cysteamine and CTAB modified AuNPs, with an average size of 26.4 and 38.7 nm, respectively, using the seed mediated growth synthesis process (Jana et al., 2001; Niidome et al., 2004) focusing on diversely positive charge functionalized AuNPs that can be loaded on negatively charged bacteria leading to colorimetric labeling to target bacteria. Wu et al., (Zhengzong Wu, He, Cui, & Jin, 2018) designed a dual mode aptasensor for the detection of *P. aeruginosa* in chicken meat using a modification of the seed growth citrate reduction method (Xia, Xiahou, Zhang, Ding, & Wang, 2016). AuNPs 30 nm in diameter were used to carry the aptamer representing color signal probes, while cDNA - AuNPs 15 nm in diameter served as SERS signaling probes.

7. Other foods

Most Au NPs colorimetric biosensors for the detection of pathogenic bacteria are reported for milk and meat but other foods and water have also been tested. The assays are particularly efficient when performed in water samples as shown for *Salmonella* (R. Luo et al., 2014), cholera toxin produced by *Vibrio cholera* (Khan, DeGrasse, Yakes, & Croley, 2015), enterohemorrhagic *E. coli* (Jyoti, Pandey, Singh, Jain, & Shanker, 2010), *P. aeruginosa* (Das, Dhiman, Kapil, Bansal, & Sharma, 2019), and *Sh. Flexneri* (Feng et al., 2019). Nonspecific bacterial detection can be achieved using unmodified AuNPs (Du et al., 2020). The assay is dependent on the electrostatic interaction between bacteria and negatively charged AuNPs. In this case by adjusting the pH of the test solution, the efficiency is improved to enable a naked-eye visualization of untreated bacteria as shown for *S. aureus*, *S. flexneri*, *P. aeruginosa*, *V. parahaemolyticus*, *B. subtilis*, E*. coli O157:H7*, and *S. typhimurium*.

Cho et al., have compared immuno-Au NPs based *in-situ* sensor performances for detection of *E. coli* O157:H7 and *S. typhimurim* in ground beef, milk and pineapple juice (Cho & Irudayaraj, 2013). A low LoD of 3 CFU/mL was found in meat and milk while a LoD of 15 CFU/mL was found in pineapple juice. The lower sensitivity of biosensors in juice maybe due to its low pH that probably interfered with antibody-antigen interactions.

Recently, a low LoD of only 1 CFU/mL was obtained when *S. typhimurium* was detected in eggshell and egg white samples (Q. Chen, Gao, & Jia, 2021). For this, bovine serum albumin (BSA) was used to stabilize gold nanoclusters (AuNCs). Obtained BSA-AuNCs complexes possessed a strong intrinsic peroxidase-like activity and were highly stable over a wide range of pHs and temperatures. Increased sensitivity was reached by a separate modification of clusters with two aptamers that recognize *S. typhimurium* cells. The capture of *S. typhimurium* by the dual-aptamers modified BSA-AuNCs (aptamers@BSA-AuNCs@*Salmonella*) was revealed upon addition of TMB as a chromogenic substrate. The intensity of the solution blue color was proportional to the

pathogen concentration ranging from 10 CFU/mL to 10^6 CFU/mL. In another study, peroxidase-like activity of AuNPs was obtained under UV irradiation (Xie et al., 2019). Sensitive detection of *S. aureus* and its enterotoxin B was obtained using aptamer-AuNPs complexes in a 96-well plate coated with chitosan-AuNCs. In the presence of *S. aureus* the solution changed from colorless to blue upon addition of TMB (Xie et al., 2019). In this assay colored AuNPs significantly amplified the response signal enabling a distinguishable color detection of enterotoxin B with the LoD of 10^{-12} g/mL in corn, rice and flour for naked-eye readout. Compared to the conventional ELISA for enterotoxin B quantification, the proposed colorimetric strategy seemed much easier for implementation in routine food screening in a facile and low-cost manner.

Some recent results employing AuNPs-based detection strategies to detect bacteria and their toxins in water and various foods are given in Table 3. As with meat and milk, detection in other foods used AuNPs either purchased or synthesized, most commonly using modifications of the citrate reduction method, rendering AuNPs with an average size of 13 nm (Quintela et al., 2019), 15 nm (S. Wu et al., 2015), 20 nm (Khan et al., 2015), 30 nm (Cho & Irudayaraj, 2013) for different types of AuNP based tests. The influence of particle size (16, 25 and 34 nm) and different surface modifications on the catalytic reaction of AuNPs synthesized using the Frens method used for fluorescence detection was investigated by (X. Wang, Pauli, Niessner, Resch-Genger, & Knopp, 2015), showing that smaller sized particles showed higher catalytic activity.

8. Conclusions and Perspectives

AuNPs are the most popular nanomaterial used in analytical assays providing visible signal readout. Low-cost AuNPs-based biosensors designed for rapid on-site detection of foodborne pathogens attract extensive attention in the field of food control because they remarkably simplify

the procedure, and may potentially satisfy all demands of the food industry for screening tests at in-line and off-line levels. LSPR biosensors involve binding of bacteria or their toxins to AuNPs bioconjugated with recognition elements and transduction into colorimetric signals detectable to the naked eye, or a portable reader, thereby enabling extremely rapid analysis. However, actual applications of LSPR biosensors in food analysis are limited because of their low sensitivity (T. Xu & Geng, 2020). Compared to electrochemical biosensors that are reported to provide the LoD of 1 CFU/mL (Cesewski & Johnson, 2020; Vidic & Manzano, 2021), AuNPs-colorimetric biosensors are less sensitive. Tailoring the AuNPs size, shape or inter-particle distance may increase the test sensitivity. Further, coupling of the LSPR phenomenon to an enzymatic reaction (such as H_2O_2 based, peroxidase like, HRP) is a signal amplification strategy that may enable direct test application to naturally contaminated foods. Finally, to increase test sensitivity, bacterial cells or toxins can be pre-concentrated prior to analysis. Although signal amplification strategies we presented significantly increase the sensitivity of detection they increase experimental complexity and usually prolong the assay time and raise the price of analysis.

There are still some technical drawbacks to be solved to enable widespread application AuNPs-based tests. In some cases, food samples have to be pretreated using a multistep procedure before detection to eliminate the matrix effect. Furthermore, AuNP-based tests, including the most popular lateral flow assays, are not easily integrated in devices and can provide a single signal output. It is expected that future development will include novel highly sensitive detection without additional amplification steps, and integration of differently functionalized AuNPs into a multicolor biosensor for multiplex pathogen detection. Despite many technical challenges, rapid development of AuNPs based biosensors ensures future application of LSPR sensors in the food field.

Acknowledgment

We thank Thierry Meylheuc for his expertise and the MIMA2 platform for access to electron microscopy equipment (MIMA2, INRAE, 2018. Microscopy and Imaging Facility for Microbes, Animals and Foods, https://doi.org/10.15454/1.5572348210007727E12) and Mayura Subramaniam (Université Paris-Saclay) for technical assistance. This research was supported in part by the European Union's Horizon 2020 research and innovation programme under the Marie Skłodowska–Curie grant agreement N° 872662 (IPANEMA) to MM and JV. MVN acknowledges support of the Ministry for Education, Science and Technological Development of the Republic of Serbia, contact 451-03-9/2021-14/200053.

Tables

Table 1. Target bacteria and their toxins, recognition elements and AuNPs-based tests used for detection in milk [§]

Target	Nanoparticles-Type of test	Recognition element	Visualization	Limit of detection (LOD)	Reference
Bacteria					
C. jejuni	Au@Pd - enzymatic reaction	Aptamer	Naked eyes	100 CFU/mL	(Dehghani et al., 2018)
Cronobacker sakazakii	AuNPs - colorimetric test	Aptamer	Naked eyes	$7.1x10^3$ CFU/mL	(H.-S. Kim et al., 2017)
Salmonella	AuNPs-MNCs-LFI*	Antibody	Image processing/ Naked eyes	10^3 CFU/mL	(Hwang et al., 2016)
Salmonella	AuNPs-SYBR green	Aptamer	Naked eyes	10 CFU/mL	(Z. Fang, Wu, Lu, & Zeng, 2014)
S. typhimurium	AuNPs - colorimetric test	Dual aptamers	Naked eyes	95 CFU/mL	(S. Chen et al., 2020)
S. typhimurium	AuNPs - colorimetric test	Aptamer	Naked eyes	72 CFU/mL	(Ma et al., 2017)
S. typhimurium	MNPs*-AuNPs- sandwich assay	Aptamer	Naked eyes	$1.9x10^2$ CFU/mL	(Duan et al., 2016)
S. typhimurium	AuNPs - ELAAS*	Antibody; Aptamer	UV-vis	10^3 CFU/mL	(W. Wu et al., 2014)
Salmonella	AuNPs-LAMP-LPD*	Antibody	Naked eyes	/	(Zhao et al., 2017)
S. aureus	AuNPs colorimetric array coupled with TSA*	Aptamer	Plate reader	9 CFU/mL	(Yuan et al., 2014)
P. aeruginosa, *V. cholerae*, *E. coli*	AuNPs - colorimetric test	Phage	Naked eyes	100 cells	(Peng et al., 2020)
E. coli O157:H7	Au^{MBA*}@Ag - SERS-LFS*	Antibody	Naked eyes/biosensor	5×10^4 CFU/mL	(H. b. Liu et al., 2019)
E. coli O157:H7	MNPs-AuNPs – colorimetric test	Antibody	Naked eyes	41 CFU/mL	(X. Xu et al., 2017)
E. coli O157:H7	AuNPs	Aptamer	Strip reader	10 CFU	(W. Wu et al., 2015)

S. aureus	MNPs-AuNPs	Antibody	Naked eyes	1.5×10^{3} CFU/mL	(Sung et al., 2013)
E. coli O157:H7	AuNPs-LFI*	Antibody	Naked eyes	1.14×10^{3} CFU/mL	(M. Chen et al., 2015)
E. coli O157:H7, *Shigella boydii*	AuNPs-LFI*	Antibody	Naked eyes	4 CFU/mL	(Song et al., 2016)
Cronobacter sakazakii	AuNPs	Antibody	Naked eyes	10^{3} CFU/mL	(Pan et al., 2018)
Toxins					
Melamine	AuNPs colorimetric test	/	Naked eyes	0.5 mg/L	(Kumar et al., 2014)
Staphylococcal enterotoxin A	AuNPs -colorimetric tets	Antibody	Naked eyes	/	(Haddada et al., 2017)
Botulinum neurotoxin type A	AuNPs colorimetric test	Antibody	Microscopic imaging	10 pg/mL	(Cheng & Chuang, 2019)
Staphylococcal enterotoxin B	AuNR@Pt – fluorescent test	Aptamer	Spectrophotometer	0.9 pg/mL	(Zhengzong Wu, He, & Cui, 2018)
Staphylococcal enterotoxin B	AuNPs – colorimetric test	Aptamer	Naked eyes	0.5 ng/mL	(Mondal, Ramlal, Lavu, & Kingston, 2018)
Staphylococcal enterotoxin B	Magnetic gold nanorod	Peptid	SERS	2.2×10^{-16} M	(Temur et al., 2012)

*AuNPs= Gold Nanoparticles; MNCs= Magnetic Nanoparticle clusters; LAMP= Loop-mediated isothermal amplification; LDP= Lateral Flow Dipstick; LFI= Lateral Flow Immunoassay; MNPs= Magnetic Nanoparticles; SERS-surface enhanced Raman Spectroscopy; TMB=3,3',5,5'-tetramethylbenzidine.

[§]Note: Studies presented are from the past 10 years.

Table 2. Target bacteria, recognition elements and AuNPs-based tests used for detection in meat[§]

Bacteria	Type of test	Recognition element	Visualization	Limit of detection (LOD)	Reference
L. monocytogenes	LAMP-AuNPs colorimetric test	DNA probe	Naked eyes	2.82 CFU/mL	(Wachiralurpan et al., 2018)
E.coli, L. monocytogenes Salmonella spp.	AuNPs colorimetric test	Aptamers	Naked eyes	10^5 CFU/mL	(Ledlod et al., 2020)
C. jejuni, C. coli	AuNPs colorimetric test	Aptamers	Naked eyes	$7.2x10^5$ CFU/mL	(Y.-J. Kim et al., 2018)
C. jejuni	RNAse H activity-AuNPs colorimetric test	RNAse H	Naked eyes	1.2 pM	(McVey, Huang, Elliott, & Cao, 2017)
Salmonella spp.	IMS - AuNPs colorimetric test	DNA probe	Naked eyes	10 CFU/mL	(Quintela et al., 2019)
E.coli O157:H7 *S. thyphymurium*	IMS-AuNPs-ELISA	Antibodies	Microplate reader	15 CFU/mL 3 CFU/mL	(Cho & Irudayaraj, 2013)
E. coli O157:H7 *S. enteritidis*	AuNPs@-LFS colorimetric assay	Antibody	Naked eyes	10^3-10^4 CFU/mL	(Bu et al., 2019)
E. coli O157:H7	Au^{MBA*}@Ag - SERS-LFS*	Antibody	Naked eyes/biosensor	5×10^4 CFU/mL	(H. b. Liu et al., 2019)
E. coli O157:H7	AuNPs-GQDs*-	DNA probe	Spectrophotometer	1.1 ± 0.6 nM	(Saad et al., 2019)
P. aeruginosa	AuNPs – colorimetric test / SERS	Aptamer/DNA probe	Naked eyes/Spectrophotometer	/	(Zhengzong Wu, Deyun He, Bo Cui, et al., 2018)

*, LFS- Lateral Flow Strips; GQDs -Graphene Quantum Dots;

[§]Note: Studies presented are from the past 10 years.

Table 3. Target bacteria and their toxins, recognition elements and AuNPs-based tests used for detection in water and other matrices[§]

Target	Type of test	Recognition element	Visualization	Limit of detection (LOD)	Matrix	Reference
E. coli P. aeruginosa V. choleare	AuNPs colorimetric test	Phage	Naked eyes	100 cells	Seawater	(Peng et al., 2020)
V. parahaemolyticus	MNPs-AuNPs enzymatic colorimetric assay	Aptamer	Naked eyes	10 CFU/mL	Ground water, sea water, waste water	(S. Wu et al., 2015)
Salmonella spp.	IMS-AuNPs colorimetric test	DNA probe	Naked eyes	10 CFU/mL	Chicken meat; blueberries	(Quintela et al., 2019)
E.coli O157:H7 *S. thyphymurium*	IMS-AuNPs-ELISA	Antibodies	Microplate reader	15 CFU/mL 3 CFU/mL	Fat milk; ground beef; pineapple juice	(Cho & Irudayaraj, 2013)
E.coli O157:H7	AuNPs - colorimetric test	Antibody	Naked eyes	/	Yellow corn	(Ali, Eldin, Moghazy, Tork, & Omara, 2014)
E.coli O157:H7 *S. enteritidis*	AuNPs@-LFS colorimetric assay	Antibody	Naked eyes	10^3-10^4 CFU/mL	Water; lettuce; pork	(Bu et al., 2019)
Shigella flexneri	AuNPs colorimetric test	Aptamer	Naked eyes	$1.50x10^2$ CFU/mL	Smoked salmon	(Q. Fang et al., 2019)
B. cereus	AuNPs –LFA*	Phage cell wall binding domain	Naked eyes	$1×10^4$ CFU/mL	buffer	(Kong, Shin, Heu, Park, & Ryu, 2017)
Shiga toxin-producing *E. coli*	AuNPs-LFA*	Aptamer	Naked eyes	/	Bacterial medium	(Silva et al., 2019)
Toxins						
Melamine	AuNPs – colorimetric assay	Antibody	Spectrophotometer	0.88 µM	Maize	(X. Wang et al., 2015)
Pyocyanin	AuNPs-gold coated zein film	/	SERS	25 µM	Drinking water	(Jia et al., 2019)
Shiga-like Toxin 1	AuNPs@PEW*	/	MALDI	40 pM	Ham	(C.-H. Li, Bai, Selvaprakash, Mong, & Chen, 2017)
Cholera toxin	AuNPs colorimetric aggregation	Antibody	UV-Vis spectrophotometer	10 nM	Lake water	(Khan et al., 2015)

* LFA –lateral flow assay; PWE -Pigeon egg white.

[§]Note: Studies presented are from the past 10 years.

Figure legends:

Figure 1.

The mechanism for the detection of foodborne and waterborne bacteria and their toxins is mainly based on analyte-induced aggregation and disaggregation AuNPs. a) A red color aqueous solution of AuNPs contains stabilized nanoparticles (diameter 20 nm), while upon salt addition, the solution changes color to blue and contains aggregated nanoparticles as observed by scanning electron microscopy. The two solutions have distinct adsorption maximums at 520nm (red) and 630 nm (blue). b) Schema of plasmon oscillation for a sphere, showing the behavior of metallic nanospheres in an external electric field. c) DNA (aptamer) in a solution prevents AuNPs aggregation in a concentration-dependent manner.

Figure 2.

Schematic illustration of a one-stage (A) and two-stage colorimetric platform (B) designed to detect bacterial cells using AuNPs and aptamers.

Figure 3.

Schematic presentation of *V. parahaemolyticus* detection by a colorimetric aptasensor based on HRP enzymatic reaction (S. Wu et al., 2015). AuNPs modified with horseradish peroxidase (HRP) enzyme and the first specific aptamer (Apt1) together with magnetic nanoparticles (MNPs) carrying the second specific aptamer (Apt2) are added to the sample. Bacterial cells with attached AuNPs-Apt1 and MNP-Apt2 are collected using an external magnet and washed to eliminate the matrix. After addition of the HRP substrate TMB, and the activator H_2O_2 a blue colored reaction product is formed signaling the presence of the pathogen.

Figure 4.

Schematic representation of the lateral flow test showing movement of a sample and aptamer labeled AuNPs across the strip providing a positive or negative result.

Figure 5.

Schematic illustration of a streptavidin magnetic beads (SMBs)-aptamer sandwich based colorimetric sensor for detection of *S. typhimurium* in milk. Adapted with permission from (S. Chen et al., 2020).

Figure 6.

A) Schematic illustration of a LAMP-AuNPs/DNA probe assay. Adapted with permission from (Wachiralurpan et al., 2018). B) The operating principle of a colorimetric biosensor for detection of *E. coli* O157:H7 based on AuNPs aggregation and smart phone imaging. Adapted with permission from (Zheng et al., 2019).

References:

Aldewachi, H., Chalati, T., Woodroofe, M., Bricklebank, N., Sharrack, B., & Gardiner, P. (2018). Gold nanoparticle-based colorimetric biosensors. *Nanoscale, 10*(1), 18-33.

Ali, M., Eldin, T. S., Moghazy, G., Tork, I. M., & Omara, I. (2014). Detection of E. coli O157: H7 in feed samples using gold nanoparticles sensor. *Int. J. Curr. Microbiol. App. Sci, 3*(6), 697-708.

Authority, E. F. S., Prevention, E. C. f. D., & Control. (2018). The European Union summary report on trends and sources of zoonoses, zoonotic agents and food-borne outbreaks in 2017. *EFSa Journal, 16*(12), e05500.

Balbinot, S., Srivastav, A. M., Vidic, J., Abdulhalim, I., & Manzano, M. (2021). Plasmonic biosensors for food control. *Trends in Food Science & Technology*.

Bastús, N. G., Comenge, J., & Puntes, V. (2011). Kinetically controlled seeded growth synthesis of citrate-stabilized gold nanoparticles of up to 200 nm: size focusing versus Ostwald ripening. *Langmuir, 27*(17), 11098-11105.

Bloomfield, V., & Crothers, D. M. (2000). *Nucleic acids: structures, properties and functions*.

Bu, T., Jia, P., Liu, J., Liu, Y., Sun, X., Zhang, M., . . . Wang, L. (2019). Diversely positive-charged gold nanoparticles based biosensor: A label-free and sensitive tool for foodborne pathogen detection. *Food chemistry: X, 3*, 100052.

Byzova, N. A., Safenkova, I. V., Slutskaya, E. S., Zherdev, A. V., & Dzantiev, B. B. (2017). Less is more: A comparison of antibody–gold nanoparticle conjugates of different ratios. *Bioconjugate chemistry, 28*(11), 2737-2746.

Cao, G., Li, K., Guo, J., Lu, M., Hong, Y., & Cai, Z. (2020). Mass Spectrometry for Analysis of Changes during Food Storage and Processing. *Journal of Agricultural and Food Chemistry, 68*(26), 6956-6966.

Cesewski, E., & Johnson, B. N. (2020). Electrochemical biosensors for pathogen detection. *Biosensors and Bioelectronics*, 112214.

Chang, C.-C., Chen, C.-P., Wu, T.-H., Yang, C.-H., Lin, C.-W., & Chen, C.-Y. (2019). Gold nanoparticle-based colorimetric strategies for chemical and biological sensing applications. *Nanomaterials, 9*(6), 861.

Chen, M., Yu, Z., Liu, D., Peng, T., Liu, K., Wang, S., . . . Lai, W. (2015). Dual gold nanoparticle lateflow immunoassay for sensitive detection of Escherichia coli O157: H7. *Analytica Chimica Acta, 876*, 71-76.

Chen, Q., Gao, R., & Jia, L. (2021). Enhancement of the peroxidase-like activity of aptamers modified gold nanoclusters by bacteria for colorimetric detection of Salmonella typhimurium. *Talanta, 221*, 121476.

Chen, S., Yang, X., Fu, S., Qin, X., Yang, T., Man, C., & Jiang, Y. (2020). A novel AuNPs colorimetric sensor for sensitively detecting viable Salmonella typhimurium based on dual aptamers. *Food Control*, 107281.

Cheng, H.-P., & Chuang, H.-S. (2019). Rapid and Sensitive Nano-Immunosensors for Botulinum. *ACS sensors, 4*(7), 1754-1760.

Cho, I.-H., & Irudayaraj, J. (2013). In-situ immuno-gold nanoparticle network ELISA biosensors for pathogen detection. *International journal of food microbiology, 164*(1), 70-75.

Choi, J. R., Yong, K. W., Choi, J. Y., & Cowie, A. C. (2019). Emerging point-of-care technologies for food safety analysis. *Sensors, 19*(4), 817.

Das, R., Dhiman, A., Kapil, A., Bansal, V., & Sharma, T. K. (2019). Aptamer-mediated colorimetric and electrochemical detection of Pseudomonas aeruginosa utilizing peroxidase-mimic activity of gold NanoZyme. *Analytical and bioanalytical chemistry, 411*(6), 1229-1238.

de Puig, H., Bosch, I., Carré-Camps, M., & Hamad-Schifferli, K. (2017). Effect of the protein corona on antibody–antigen binding in nanoparticle sandwich immunoassays. *Bioconjugate chemistry, 28*(1), 230-238.

Dehghani, Z., Hosseini, M., Mohammadnejad, J., Bakhshi, B., & Rezayan, A. H. (2018). Colorimetric aptasensor for Campylobacter jejuni cells by exploiting the peroxidase like activity of Au@ Pd nanoparticles. *Microchimica Acta, 185*(10), 448.

Deisingh, A. K., & Thompson, M. (2002). Detection of infectious and toxigenic bacteria. *Analyst, 127*(5), 567-581.

Dewey-Mattia, D., Manikonda, K., Hall, A. J., Wise, M. E., & Crowe, S. J. (2018). Surveillance for foodborne disease outbreaks—United States, 2009–2015. *MMWR Surveillance Summaries, 67*(10), 1.

Dincer, C., Bruch, R., Costa-Rama, E., Fernández-Abedul, M. T., Merkoçi, A., Manz, A., . . . Güder, F. (2019). Disposable sensors in diagnostics, food, and environmental monitoring. *Advanced Materials, 31*(30), 1806739.

Domínguez, I., Frenich, A. G., & Romero-González, R. (2020). Mass spectrometry approaches to ensure food safety. *Analytical Methods, 12*(9), 1148-1162.

Dong, J., Carpinone, P. L., Pyrgiotakis, G., Demokritou, P., & Moudgil, B. M. (2020). Synthesis of precision gold nanoparticles using Turkevich method. *KONA Powder and Particle Journal, 37*, 224-232.

Du, J., Yu, Z., Hu, Z., Chen, J., Zhao, J., & Bai, Y. (2020). A low pH-based rapid and direct colorimetric sensing of bacteria using unmodified gold nanoparticles. *Journal of Microbiological Methods, 180*, 106110.

Duan, N., Xu, B., Wu, S., & Wang, Z. (2016). Magnetic nanoparticles-based aptasensor using gold nanoparticles as colorimetric probes for the detection of Salmonella Typhimurium. *Analytical Sciences, 32*(4), 431-436.

Duqué, B., Haddad, N., Rossero, A., Membré, J.-M., & Guillou, S. (2019). Influence of cell history on the subsequent inactivation of Campylobacter jejuni during cold storage under modified atmosphere. *Food microbiology, 84*, 103263.

Elghanian, R., Storhoff, J. J., Mucic, R. C., Letsinger, R. L., & Mirkin, C. A. (1997). Selective colorimetric detection of polynucleotides based on the distance-dependent optical properties of gold nanoparticles. *Science, 277*(5329), 1078-1081.

Fang, Q., Li, Y., Miao, X., Zhang, Y., Yan, J., Yu, T., & Liu, J. (2019). Sensitive detection of antibiotics using aptamer conformation cooperated enzyme-assisted SERS technology. *Analyst, 144*(11), 3649-3658.

Fang, Z., Wu, W., Lu, X., & Zeng, L. (2014). Lateral flow biosensor for DNA extraction-free detection of salmonella based on aptamer mediated strand displacement amplification. *Biosensors and Bioelectronics, 56*, 192-197.

Feng, J., Shen, Q., Wu, J., Dai, Z., & Wang, Y. (2019). Naked-eyes detection of Shigella flexneri in food samples based on a novel gold nanoparticle-based colorimetric aptasensor. *Food Control, 98*, 333-341.

Frens, G. (1973). Controlled nucleation for the regulation of the particle size in monodisperse gold suspensions. *Nature physical science, 241*(105), 20-22.

Gao, J., Huang, X., Liu, H., Zan, F., & Ren, J. (2012). Colloidal stability of gold nanoparticles modified with thiol compounds: bioconjugation and application in cancer cell imaging. *Langmuir, 28*(9), 4464-4471.

García-Álvarez, R., Hadjidemetriou, M., Sánchez-Iglesias, A., Liz-Marzán, L. M., & Kostarelos, K. (2018). In vivo formation of protein corona on gold nanoparticles. The effect of their size and shape. *Nanoscale, 10*(3), 1256-1264.

Giljohann, D. A., Seferos, D. S., Daniel, W. L., Massich, M. D., Patel, P. C., & Mirkin, C. A. (2020). Gold nanoparticles for biology and medicine. *Spherical Nucleic Acids*, 55-90.

Grabar, K. C., Freeman, R. G., Hommer, M. B., & Natan, M. J. (1995). Preparation and characterization of Au colloid monolayers. *Analytical chemistry, 67*(4), 735-743.

Haddada, M. B., Hu, D., Salmain, M., Zhang, L., Peng, C., Wang, Y., . . . Boujday, S. (2017). Gold nanoparticle-based localized surface plasmon immunosensor for staphylococcal enterotoxin A (SEA) detection. *Analytical and bioanalytical chemistry, 409*(26), 6227-6234.

Hauser, E. A., & Lynn, J. E. (1940). *Experiments in colloid chemistry*: McGraw-Hill Book Company, Incorporated.

Hianik, T., Ostatná, V., Sonlajtnerova, M., & Grman, I. (2007). Influence of ionic strength, pH and aptamer configuration for binding affinity to thrombin. *Bioelectrochemistry, 70*(1), 127-133.

Hwang, J., Kwon, D., Lee, S., & Jeon, S. (2016). Detection of Salmonella bacteria in milk using gold-coated magnetic nanoparticle clusters and lateral flow filters. *Rsc Advances, 6*(54), 48445-48448.

Jana, N. R., Gearheart, L., & Murphy, C. J. (2001). Seeding growth for size control of 5− 40 nm diameter gold nanoparticles. *Langmuir, 17*(22), 6782-6786.

Jia, F., Barber, E., Turasan, H., Seo, S., Dai, R., Liu, L., . . . Kokini, J. L. (2019). Detection of pyocyanin using a new biodegradable SERS biosensor fabricated using gold coated zein nanostructures further decorated with gold nanoparticles. *Journal of Agricultural and Food Chemistry, 67*(16), 4603-4610.

Jiang, H., Materon, E. M., Sotomayor, M. D. P. T., & Liu, J. (2013). Fast assembly of non-thiolated DNA on gold surface at lower pH. *Journal of colloid and interface science, 411*, 92-97.

Jyoti, A., Pandey, P., Singh, S. P., Jain, S. K., & Shanker, R. (2010). Colorimetric detection of nucleic acid signature of shiga toxin producing Escherichia coli using gold nanoparticles. *Journal of nanoscience and nanotechnology, 10*(7), 4154-4158.

Khan, S. A., DeGrasse, J. A., Yakes, B. J., & Croley, T. R. (2015). Rapid and sensitive detection of cholera toxin using gold nanoparticle-based simple colorimetric and dynamic light scattering assay. *Analytica Chimica Acta, 892*, 167-174.

Khateb, H., Klös, G., Meyer, R. L., & Sutherland, D. S. (2020). Development of a label-free LSPR-Apta sensor for Staphylococcus aureus detection. *ACS Applied Bio Materials, 3*(5), 3066-3077.

Kim, H.-S., Kim, Y.-J., Chon, J.-W., Kim, D.-H., Yim, J.-H., Kim, H., & Seo, K.-H. (2017). Two-stage label-free aptasensing platform for rapid detection of Cronobacter sakazakii in powdered infant formula. *Sensors and Actuators B: Chemical, 239*, 94-99.

Kim, Y.-J., Kim, H.-S., Chon, J.-W., Kim, D.-H., Hyeon, J.-Y., & Seo, K.-H. (2018). New colorimetric aptasensor for rapid on-site detection of Campylobacter jejuni and Campylobacter coli in chicken carcass samples. *Analytica Chimica Acta, 1029*, 78-85.

Kim, Y. S., Kim, J. H., Kim, I. A., Lee, S. J., & Gu, M. B. (2011). The affinity ratio—its pivotal role in gold nanoparticle-based competitive colorimetric aptasensor. *Biosensors and Bioelectronics, 26*(10), 4058-4063.

Kim, Y. S., Kim, J. H., Kim, I. A., Lee, S. J., Jurng, J., & Gu, M. B. (2010). A novel colorimetric aptasensor using gold nanoparticle for a highly sensitive and specific detection of oxytetracycline. *Biosensors and Bioelectronics, 26*(4), 1644-1649.

Kimling, J., Maier, M., Okenve, B., Kotaidis, V., Ballot, H., & Plech, A. (2006). Turkevich method for gold nanoparticle synthesis revisited. *The Journal of Physical Chemistry B, 110*(32), 15700-15707.

Kong, M., Shin, J. H., Heu, S., Park, J.-K., & Ryu, S. (2017). Lateral flow assay-based bacterial detection using engineered cell wall binding domains of a phage endolysin. *Biosensors and Bioelectronics, 96*, 173-177.

Kotsiri, Z., Vantarakis, A., Rizzotto, F., Kavanaugh, D., Ramarao, N., & Vidic, J. (2019). Sensitive Detection of E. coli in Artificial Seawater by Aptamer-Coated Magnetic Beads and Direct PCR. *Applied Sciences, 9*(24), 5392.

Kumar, N., Seth, R., & Kumar, H. (2014). Colorimetric detection of melamine in milk by citrate-stabilized gold nanoparticles. *Analytical biochemistry, 456*, 43-49.

Law, J. W.-F., Ab Mutalib, N.-S., Chan, K.-G., & Lee, L.-H. (2015). Rapid methods for the detection of foodborne bacterial pathogens: principles, applications, advantages and limitations. *Frontiers in microbiology, 5*, 770.

Ledlod, S., Areekit, S., Santiwatanakul, S., & Chansiri, K. (2020). Colorimetric aptasensor for detecting Salmonella spp., Listeria monocytogenes, and Escherichia coli in meat samples. *Food Science and Technology International*, 1082013219899593.

Li, C.-H., Bai, Y.-L., Selvaprakash, K., Mong, K.-K. T., & Chen, Y.-C. (2017). Selective detection of Shiga-like toxin 1 from complex samples using pigeon ovalbumin functionalized gold nanoparticles as affinity probes. *Journal of Agricultural and Food Chemistry, 65*(21), 4359-4365.

Li, F., Li, F., Yang, G., Aguilar, Z. P., Lai, W., & Xu, H. (2018). Asymmetric polymerase chain assay combined with propidium monoazide treatment and unmodified gold nanoparticles for colorimetric detection of viable emetic Bacillus cereus in milk. *Sensors and Actuators B: Chemical, 255*, 1455-1461.

Li, H., & Rothberg, L. (2004). Colorimetric detection of DNA sequences based on electrostatic interactions with unmodified gold nanoparticles. *Proceedings of the National Academy of Sciences, 101*(39), 14036-14039.

Li, H., & Rothberg, L. J. (2004). Label-free colorimetric detection of specific sequences in genomic DNA amplified by the polymerase chain reaction. *Journal of the American Chemical Society, 126*(35), 10958-10961.

Lin, Z., & He, L. (2019). Recent advance in SERS techniques for food safety and quality analysis: a brief review. *Current Opinion in Food Science, 28*, 82-87.

Liu, H. b., Chen, C. y., Zhang, C. n., Du, X. j., Li, P., & Wang, S. (2019). Functionalized AuMBA@ Ag nanoparticles as an optical and SERS dual probe in a lateral flow strip for the quantitative detection of Escherichia coli O157: H7. *Journal of food science, 84*(10), 2916-2924.

Liu, X., Wang, Y., Chen, P., Wang, Y., Zhang, J., Aili, D., & Liedberg, B. (2014). Biofunctionalized gold nanoparticles for colorimetric sensing of botulinum neurotoxin a light chain. *Analytical chemistry, 86*(5), 2345-2352.

Lund, B. M. (2015). Microbiological food safety for vulnerable people. *International journal of environmental research and public health, 12*(8), 10117-10132.

Luo, R., Li, Y., Lin, X., Dong, F., Zhang, W., Yan, L., . . . Ding, S. (2014). A colorimetric assay method for invA gene of Salmonella using DNAzyme probe self-assembled gold nanoparticles as single tag. *Sensors and Actuators B: Chemical, 198*, 87-93.

Luo, Y., Xu, J., Li, Y., Gao, H., Guo, J., Shen, F., & Sun, C. (2015). A novel colorimetric aptasensor using cysteamine-stabilized gold nanoparticles as probe for rapid and specific detection of tetracycline in raw milk. *Food Control, 54*, 7-15.

Ma, X., Song, L., Zhou, N., Xia, Y., & Wang, Z. (2017). A novel aptasensor for the colorimetric detection of S. typhimurium based on gold nanoparticles. *International journal of food microbiology, 245*, 1-5.

Marathe, S. A., Chowdhury, R., Bhattacharya, R., Nagarajan, A. G., & Chakravortty, D. (2012). Direct detection of Salmonella without pre-enrichment in milk, ice-cream and fruit juice by PCR against hilA gene. *Food Control, 23*(2), 559-563.

McVey, C., Huang, F., Elliott, C., & Cao, C. (2017). Endonuclease controlled aggregation of gold nanoparticles for the ultrasensitive detection of pathogenic bacterial DNA. *Biosensors and Bioelectronics, 92*, 502-508.

Mirkin, C. A., Letsinger, R. L., Mucic, R. C., & Storhoff, J. J. (1996). A DNA-based method for rationally assembling nanoparticles into macroscopic materials. *Nature, 382*(6592), 607-609.

Mondal, B., Ramlal, S., Lavu, P. S., & Kingston, J. (2018). Highly sensitive colorimetric biosensor for Staphylococcal enterotoxin B by a label-free aptamer and gold nanoparticles. *Frontiers in microbiology, 9*, 179.

Motl, N., Smith, A., DeSantis, C., & Skrabalak, S. (2014). Engineering plasmonic metal colloids through composition and structural design. *Chemical Society Reviews, 43*(11), 3823-3834.

Nicolo, M. S., Gioffre, A., Carnazza, S., Platania, G., Silvestro, I. D., & Guglielmino, S. P. P. (2011). Viable but nonculturable state of foodborne pathogens in grapefruit juice: a study of laboratory. *Foodborne Pathogens and Disease, 8*(1), 11-17.

Niidome, T., Nakashima, K., Takahashi, H., & Niidome, Y. (2004). Preparation of primary amine-modified gold nanoparticles and their transfection ability into cultivated cells. *Chemical Communications*(17), 1978-1979.

Oh, S. Y., Heo, N. S., Shukla, S., Cho, H.-J., Vilian, A. E., Kim, J., . . . Huh, Y. S. (2017). Development of gold nanoparticle-aptamer-based LSPR sensing chips for the rapid detection of Salmonella typhimurium in pork meat. *Scientific reports, 7*(1), 1-10.

Oliver, S. P., Jayarao, B. M., & Almeida, R. A. (2005). Foodborne pathogens in milk and the dairy farm environment: food safety and public health implications. *Foodbourne Pathogens & Disease, 2*(2), 115-129.

Pan, R., Jiang, Y., Sun, L., Wang, R., Zhuang, K., Zhao, Y., . . . Man, C. (2018). Gold nanoparticle-based enhanced lateral flow immunoassay for detection of Cronobacter sakazakii in powdered infant formula. *Journal of dairy science, 101*(5), 3835-3843.

Paul, I. E., Kumar, D. N., Rajeshwari, A., Alex, S. A., Karthiga, D., Raichur, A. M., . . . Mukherjee, A. (2017). Detection of food contaminants by gold and silver nanoparticles. In *Nanobiosensors* (pp. 129-165): Elsevier.

Peng, H., Borg, R. E., Nguyen, A. B., & Chen, I. A. (2020). Chimeric Phage Nanoparticles for Rapid Characterization of Bacterial Pathogens: Detection in Complex Biological Samples and Determination of Antibiotic Sensitivity. *ACS sensors, 5*(5), 1491-1499.

Peng, H., & Chen, I. A. (2018). Rapid colorimetric detection of bacterial species through the capture of gold nanoparticles by chimeric phages. *ACS nano, 13*(2), 1244-1252.

Perelle, S., Dilasser, F., Malorny, B., Grout, J., Hoorfar, J., & Fach, P. (2004). Comparison of PCR-ELISA and LightCycler real-time PCR assays for detecting Salmonella spp. in milk and meat samples. *Molecular and cellular probes, 18*(6), 409-420.

Piella, J., Bastús, N. G., & Puntes, V. (2017). Size-dependent protein–nanoparticle interactions in citrate-stabilized gold nanoparticles: the emergence of the protein corona. *Bioconjugate chemistry, 28*(1), 88-97.

Pines, D., & Bohm, D. (1952). A collective description of electron interactions: II. Collective vs individual particle aspects of the interactions. *Physical Review, 85*(2), 338.

Pong, B.-K., Elim, H. I., Chong, J.-X., Ji, W., Trout, B. L., & Lee, J.-Y. (2007). New insights on the nanoparticle growth mechanism in the citrate reduction of gold (III) salt: formation of the Au nanowire intermediate and its nonlinear optical properties. *The Journal of Physical Chemistry C, 111*(17), 6281-6287.

Poshtiban, S., Javed, M. A., Arutyunov, D., Singh, A., Banting, G., Szymanski, C. M., & Evoy, S. (2013). Phage receptor binding protein-based magnetic enrichment method as an aid for real time PCR detection of foodborne bacteria. *Analyst, 138*(19), 5619-5626.

Prasad, D., & Vidyarthi, A. S. (2011). Gold nanoparticles-based colorimetric assay for rapid detection of Salmonella species in food samples. *World Journal of Microbiology and Biotechnology, 27*(9), 2227-2230.

Quesada-González, D., & Merkoçi, A. (2015). Nanoparticle-based lateral flow biosensors. *Biosensors and Bioelectronics, 73*, 47-63.

Quigley, L., O'Sullivan, O., Stanton, C., Beresford, T. P., Ross, R. P., Fitzgerald, G. F., & Cotter, P. D. (2013). The complex microbiota of raw milk. *FEMS microbiology reviews, 37*(5), 664-698.

Quintela, I. A., de los Reyes, B. G., Lin, C.-S., & Wu, V. C. (2019). Simultaneous colorimetric detection of a variety of Salmonella spp. in food and environmental samples by optical biosensing using oligonucleotide-gold nanoparticles. *Frontiers in microbiology, 10*, 1138.

Ramarao, N., Tran, S.-L., Marin, M., & Vidic, J. (2020). Advanced methods for detection of Bacillus cereus and its pathogenic factors. *Sensors, 20*(9), 2667.

Requena, R., Vargas, M., & Chiralt, A. (2018). Obtaining antimicrobial bilayer starch and polyester-blend films with carvacrol. *Food hydrocolloids, 83*, 118-133.

Saad, S. M., Abdullah, J., Abd Rashid, S., Fen, Y. W., Salam, F., & Yih, L. H. (2019). A fluorescence quenching based gene assay for Escherichia coli O157: H7 using graphene quantum dots and gold nanoparticles. *Microchimica Acta, 186*(12), 1-10.

Sajid, M., Kawde, A.-N., & Daud, M. (2015). Designs, formats and applications of lateral flow assay: A literature review. *Journal of Saudi Chemical Society, 19*(6), 689-705.

Sau, T. K., & Murphy, C. J. (2004). Room temperature, high-yield synthesis of multiple shapes of gold nanoparticles in aqueous solution. *Journal of the American Chemical Society, 126*(28), 8648-8649.

Sena-Torralba, A., Ngo, D. B., Parolo, C., Hu, L., Álvarez-Diduk, R., Bergua, J. F., . . . Merkoçi, A. (2020). Lateral flow assay modified with time-delay wax barriers as a sensitivity and signal enhancement strategy. *Biosensors and Bioelectronics, 168*, 112559.

Silva, M. A., Santos, A. R. R., Rocha, L. B., Caetano, B. A., Mitsunari, T., Santos, L. I., . . . Dos Santos, L. F. (2019). Development and validation of Shiga toxin-producing Escherichia coli immunodiagnostic assay. *Microorganisms, 7*(9), 276.

Slot, J., & Geuze, H. (1984). A method to prepare isodisperse colloidal gold sols in the size range 3–17 nm. *Ultramicroscopy, 15*(4), 383.

Sofos, J. N. (2008). Challenges to meat safety in the 21st century. *Meat science, 78*(1-2), 3-13.

Song, C., Liu, C., Wu, S., Li, H., Guo, H., Yang, B., . . . Zeng, H. (2016). Development of a lateral flow colloidal gold immunoassay strip for the simultaneous detection of Shigella boydii and Escherichia coli O157: H7 in bread, milk and jelly samples. *Food Control, 59*, 345-351.

Storhoff, J. J., Lazarides, A. A., Mucic, R. C., Mirkin, C. A., Letsinger, R. L., & Schatz, G. C. (2000). What controls the optical properties of DNA-linked gold nanoparticle assemblies? *Journal of the American Chemical Society, 122*(19), 4640-4650.

Su, H., Ma, Q., Shang, K., Liu, T., Yin, H., & Ai, S. (2012). Gold nanoparticles as colorimetric sensor: A case study on E. coli O157: H7 as a model for Gram-negative bacteria. *Sensors and Actuators B: Chemical, 161*(1), 298-303.

Sun, J., Lu, Y., He, L., Pang, J., Yang, F., & Liu, Y. (2020). Colorimetric sensor array based on gold nanoparticles: Design principles and recent advances. *TrAC Trends in Analytical Chemistry, 122*, 115754.

Sung, Y. J., Suk, H.-J., Sung, H. Y., Li, T., Poo, H., & Kim, M.-G. (2013). Novel antibody/gold nanoparticle/magnetic nanoparticle nanocomposites for immunomagnetic separation and rapid colorimetric detection of Staphylococcus aureus in milk. *Biosensors and Bioelectronics, 43*, 432-439.

Swierczewska, M., Liu, G., Lee, S., & Chen, X. (2012). High-sensitivity nanosensors for biomarker detection. *Chemical Society Reviews, 41*(7), 2641-2655.

Tao, X., Chang, X., Wan, X., Guo, Y., Zhang, Y., Liao, Z., . . . Song, E. (2020). Impact of Protein Corona on Noncovalent Molecule–Gold Nanoparticle-Based Sensing. *Analytical Chemistry, 92*(22), 14990-14998.

Temur, E., Zengin, A., Boyacı, I. s. H., Dudak, F. C., Torul, H., & Tamer, U. u. (2012). Attomole sensitivity of staphylococcal enterotoxin B detection using an aptamer-modified surface-enhanced Raman scattering probe. *Analytical chemistry, 84*(24), 10600-10606.

Turkevich, J., Stevenson, P. C., & Hillier, J. (1951). A study of the nucleation and growth processes in the synthesis of colloidal gold. *Discussions of the Faraday Society, 11*, 55-75.

Tyagi, H., Kushwaha, A., Kumar, A., & Aslam, M. (2016). A facile pH controlled citrate-based reduction method for gold nanoparticle synthesis at room temperature. *Nanoscale research letters, 11*(1), 1-11.

Verma, M. S., Rogowski, J. L., Jones, L., & Gu, F. X. (2015). Colorimetric biosensing of pathogens using gold nanoparticles. *Biotechnology advances, 33*(6), 666-680.

Vial, S., Nykypanchuk, D., Deepak, F. L., Prado, M., & Gang, O. (2014). Plasmonic response of DNA-assembled gold nanorods: Effect of DNA linker length, temperature and linker/nanoparticles ratio. *Journal of colloid and interface science, 433*, 34-42.

Vidic, J., Chaix, C., Manzano, M., & Heyndrickx, M. (2020). Food Sensing: Detection of Bacillus cereus Spores in Dairy Products. *Biosensors, 10*(3), 15.

Vidic, J., & Manzano, M. (2021). Electrochemical biosensors for rapid pathogen detection. *Current Opinion in Electrochemistry*, 100750.

Vidic, J., Vizzini, P., Manzano, M., Kavanaugh, D., Ramarao, N., Zivkovic, M., . . . Gadjanski, I. (2019). Point-of-need DNA testing for detection of foodborne pathogenic bacteria. *Sensors, 19*(5), 1100.

Vizzini, P., Braidot, M., Vidic, J., & Manzano, M. (2019). Electrochemical and optical biosensors for the detection of campylobacter and listeria: An update look. *Micromachines, 10*(8), 500.

Vizzini, P., Manzano, M., Farre, C., Meylheuc, T., Chaix, C., Ramarao, N., & Vidic, J. (2020). Highly sensitive detection of Campylobacter spp. In chicken meat using a silica nanoparticle enhanced dot blot DNA biosensor. *Biosensors and Bioelectronics, 171*, 112689.

Wachiralurpan, S., Sriyapai, T., Areekit, S., Sriyapai, P., Augkarawaritsawong, S., Santiwatanakul, S., & Chansiri, K. (2018). Rapid colorimetric assay for detection of Listeria monocytogenes in food samples using LAMP formation of DNA concatemers and gold nanoparticle-DNA probe complex. *Frontiers in Chemistry, 6*, 90.

Wang, A., Perera, Y. R., Davidson, M. B., & Fitzkee, N. C. (2016). Electrostatic interactions and protein competition reveal a dynamic surface in gold nanoparticle–protein adsorption. *The Journal of Physical Chemistry C, 120*(42), 24231-24239.

Wang, H., Dardir, K., Lee, K.-B., & Fabris, L. (2019). Impact of Protein Corona in Nanoflare-Based Biomolecular Detection and Quantification. *Bioconjugate chemistry, 30*(10), 2555-2562.

Wang, X., Pauli, J., Niessner, R., Resch-Genger, U., & Knopp, D. (2015). Gold nanoparticle-catalyzed uranine reduction for signal amplification in fluorescent assays for melamine and aflatoxin B1. *Analyst, 140*(21), 7305-7312.

Wang, Y., Zhan, L., & Huang, C. Z. (2010). One-pot preparation of dextran-capped gold nanoparticles at room temperature and colorimetric detection of dihydralazine sulfate in uric samples. *Analytical Methods, 2*(12), 1982-1988.

Wu, S., Wang, Y., Duan, N., Ma, H., & Wang, Z. (2015). Colorimetric aptasensor based on enzyme for the detection of Vibrio parahemolyticus. *Journal of Agricultural and Food Chemistry, 63*(35), 7849-7854.

Wu, W., Li, J., Pan, D., Li, J., Song, S., Rong, M., . . . Lu, J. (2014). Gold nanoparticle-based enzyme-linked antibody-aptamer sandwich assay for detection of Salmonella Typhimurium. *ACS applied materials & interfaces, 6*(19), 16974-16981.

Wu, W., Zhao, S., Mao, Y., Fang, Z., Lu, X., & Zeng, L. (2015). A sensitive lateral flow biosensor for Escherichia coli O157: H7 detection based on aptamer mediated strand displacement amplification. *Analytica chimica acta, 861*, 62-68.

Wu, Z., He, D., & Cui, B. (2018). A fluorometric assay for staphylococcal enterotoxin B by making use of platinum coated gold nanorods and of upconversion nanoparticles. *Microchimica Acta, 185*(11), 1-8.

Wu, Z., He, D., Cui, B., & Jin, Z. (2018). A bimodal (SERS and colorimetric) aptasensor for the detection of Pseudomonas aeruginosa. *Microchimica Acta, 185*(11), 1-7.

Wu, Z., Huang, X., Li, Y.-C., Xiao, H., & Wang, X. (2018). Novel chitosan films with laponite immobilized Ag nanoparticles for active food packaging. *Carbohydrate Polymers, 199*, 210-218.

Xia, H., Xiahou, Y., Zhang, P., Ding, W., & Wang, D. (2016). Revitalizing the Frens method to synthesize uniform, quasi-spherical gold nanoparticles with deliberately regulated sizes from 2 to 330 nm. *Langmuir, 32*(23), 5870-5880.

Xie, X., Tan, F., Xu, A., Deng, K., Zeng, Y., & Huang, H. (2019). UV-induced peroxidase-like activity of gold nanoclusters for differentiating pathogenic bacteria and detection of enterotoxin with colorimetric readout. *Sensors and Actuators B: Chemical, 279*, 289-297.

Xu, T., & Geng, Z. (2020). Strategies to improve performances of LSPR biosensing: Structure, materials, and interface modification. *Biosensors and Bioelectronics*, 112850.

Xu, X., Yuan, Y., Hu, G., Wang, X., Qi, P., Wang, Z., . . . Li, Y. (2017). Exploiting pH-regulated dimer-tetramer transformation of concanavalin a to develop colorimetric biosensing of bacteria. *Scientific reports, 7*(1), 1-8.

Yuan, J., Wu, S., Duan, N., Ma, X., Xia, Y., Chen, J., . . . Wang, Z. (2014). A sensitive gold nanoparticle-based colorimetric aptasensor for Staphylococcus aureus. *Talanta, 127*, 163-168.

Zhang, S.-F., Liu, L.-N., Tang, R.-H., Liu, Z., He, X.-C., Qu, Z.-G., & Li, F. (2019). Sensitivity enhancement of lateral flow assay by embedding cotton threads in paper. *Cellulose, 26*(13), 8087-8099.

Zhang, X., Liu, B., Servos, M. R., & Liu, J. (2013). Polarity control for nonthiolated DNA adsorption onto gold nanoparticles. *Langmuir, 29*(20), 6091-6098.

Zhang, X., Servos, M. R., & Liu, J. (2012). Surface science of DNA adsorption onto citrate-capped gold nanoparticles. *Langmuir, 28*(8), 3896-3902.

Zhao, Y., Jiang, X., Qu, Y., Pan, R., Pang, X., Jiang, Y., & Man, C. (2017). Salmonella detection in powdered dairy products using a novel molecular tool. *Journal of dairy science, 100*(5), 3480-3496.

Zheng, L., Cai, G., Wang, S., Liao, M., Li, Y., & Lin, J. (2019). A microfluidic colorimetric biosensor for rapid detection of Escherichia coli O157: H7 using gold nanoparticle aggregation and smart phone imaging. *Biosensors and Bioelectronics, 124*, 143-149.

A

Au NPs (diameter 20 nm)

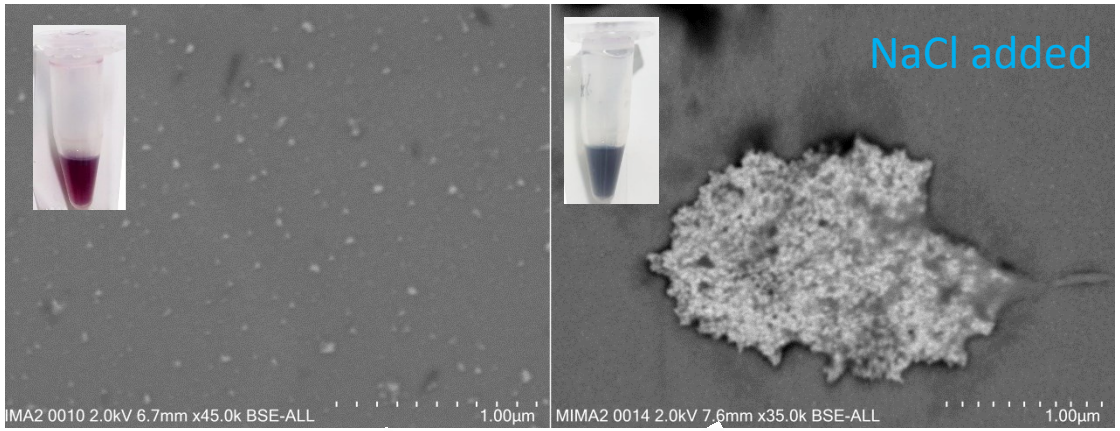

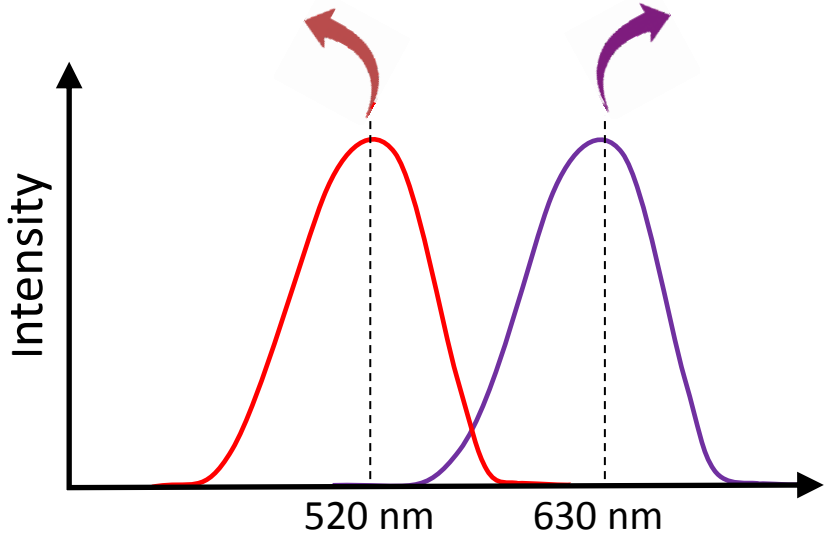

B

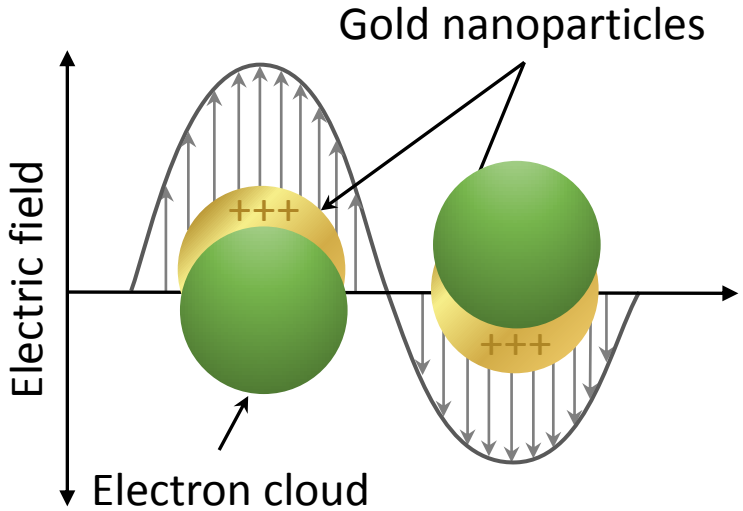

C

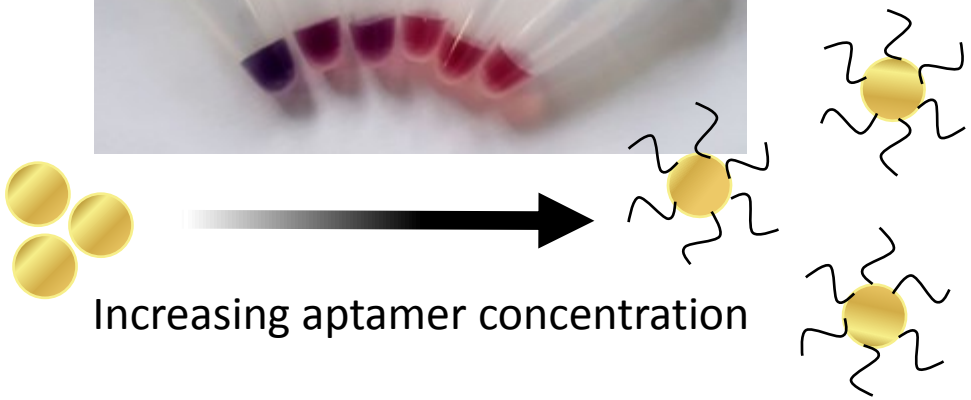

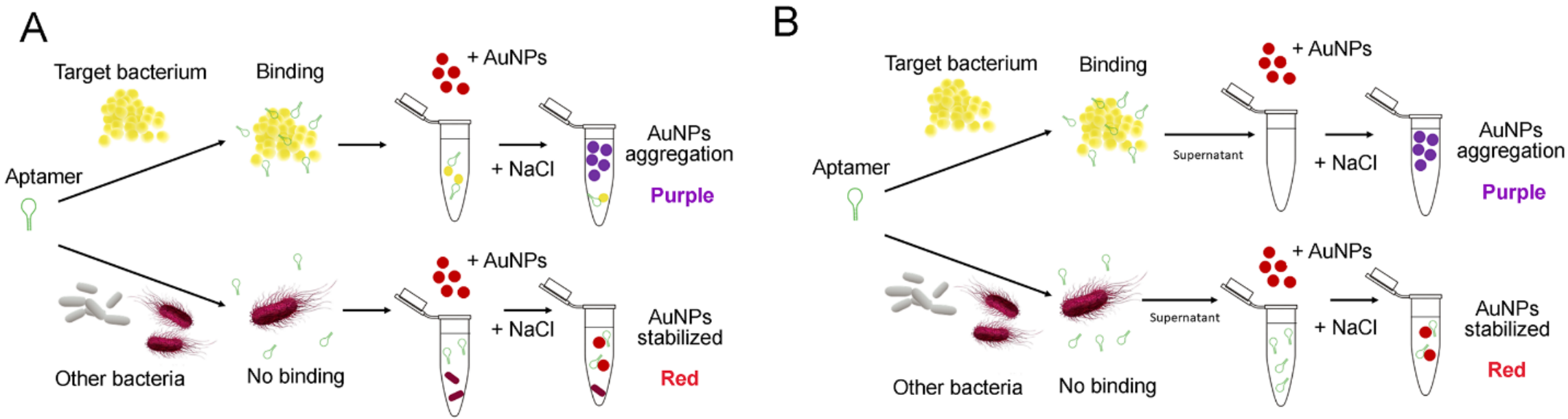
A
Target bacterium
Binding
+ AuNPs
Aptamer
+ NaCl
AuNPs
aggregation
Purple
+ AuNPs
+ NaCl
AuNPs
stabilized
Red
Other bacteria
No binding
B
Target bacterium
Binding
+ AuNPs
Supernatant
Aptamer
+ NaCl
AuNPs
aggregation
Purple
+ AuNPs
Supernatant
+ NaCl
AuNPs
stabilized
Red
Other bacteria
No binding

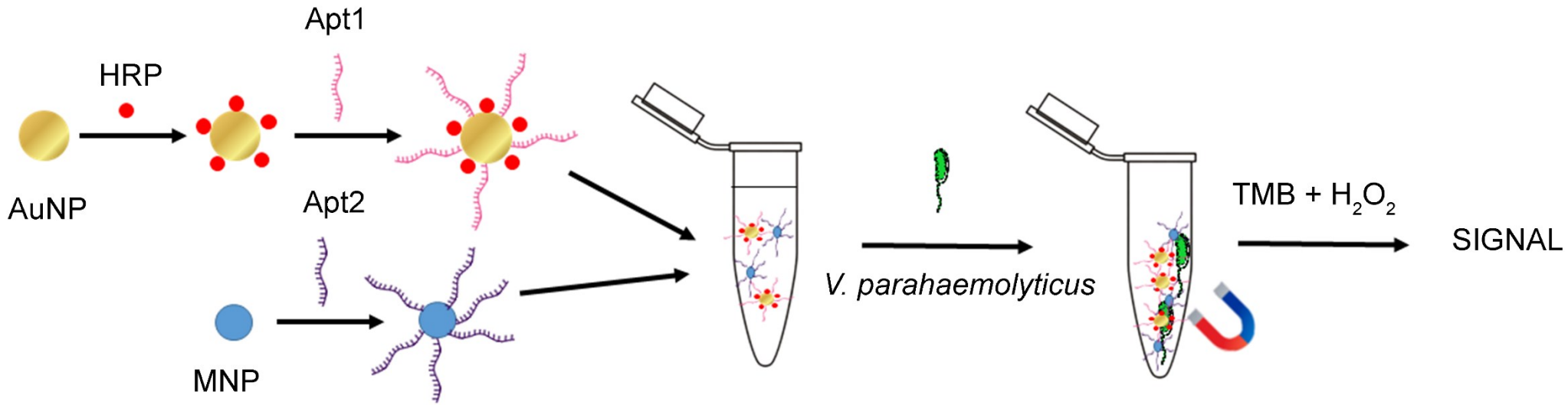
Apt1
HRP
AuNP
Apt2
MNP
V. parahaemolyticus
TMB + H_2O_2
SIGNAL

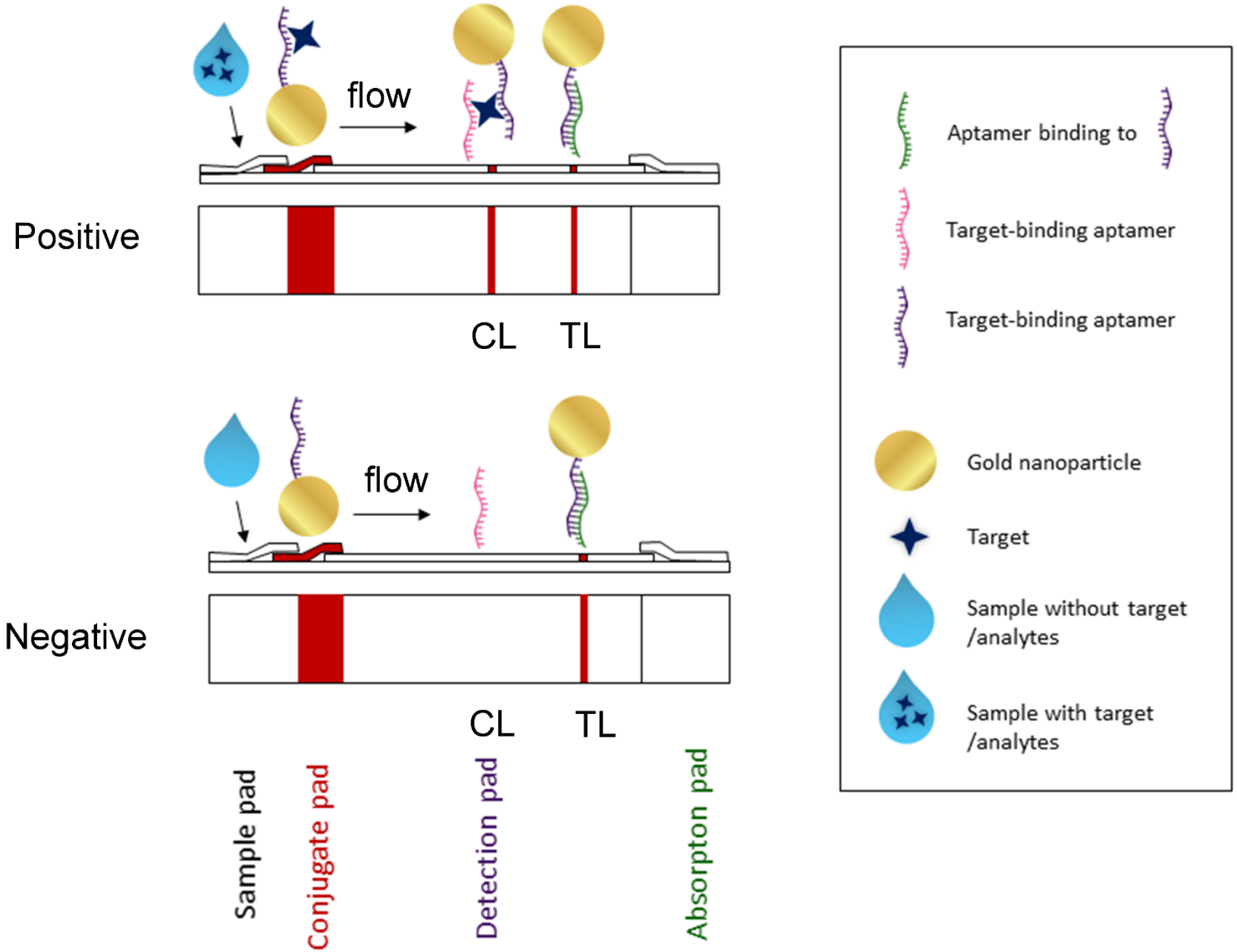
Positive
flow
CL
TL
Negative
flow
CL
TL
Sample pad
Conjugate pad
Detection pad
Absorpton pad
Aptamer binding to
Target-binding aptamer
Target-binding aptamer
Gold nanoparticle
Target
Sample without target /analytes
Sample with target /analytes

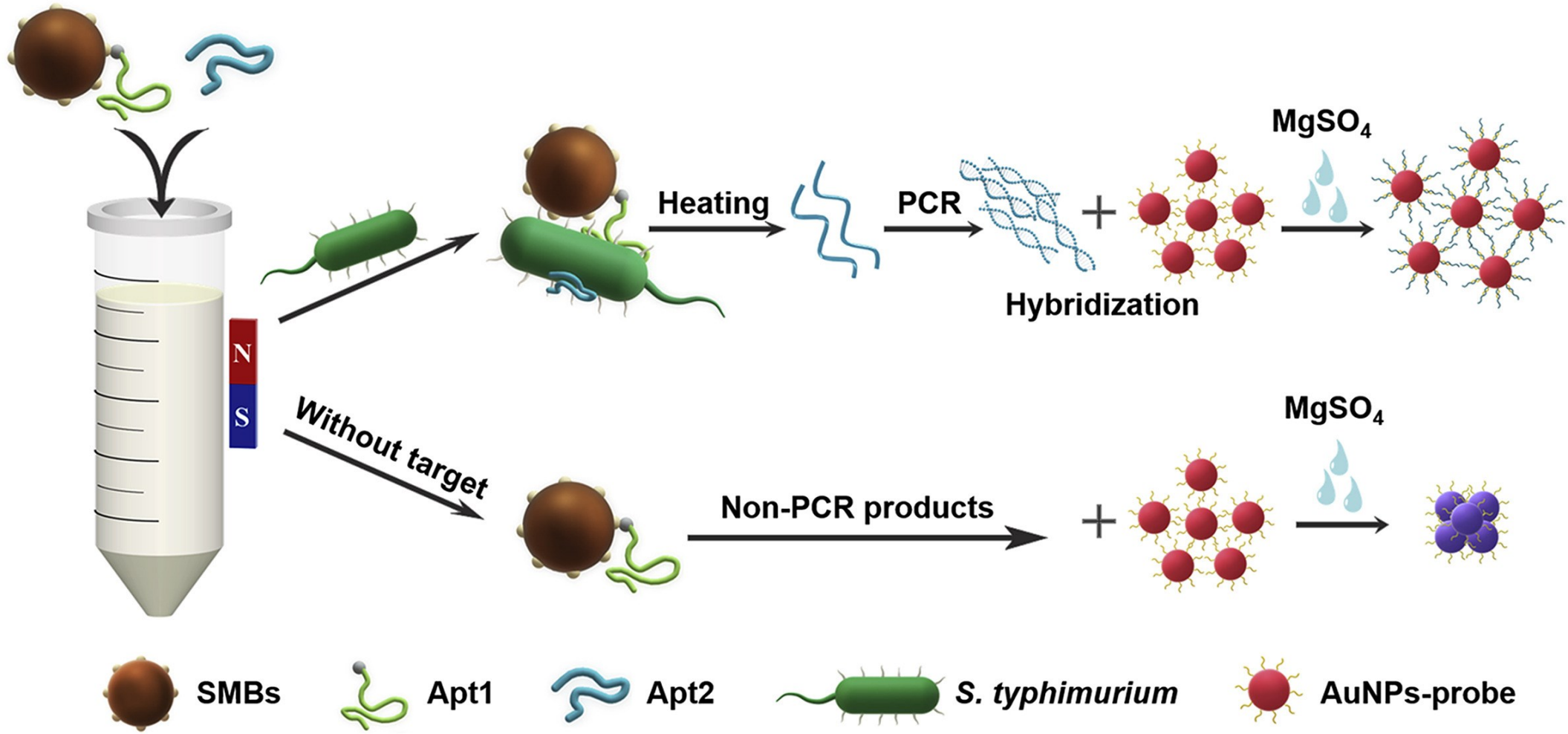
N
S
Heating
PCR
Hybridization
MgSO4
Without target
Non-PCR products
MgSO4
SMBs
Apt1
Apt2
S. typhimurium
AuNPs-probe

A

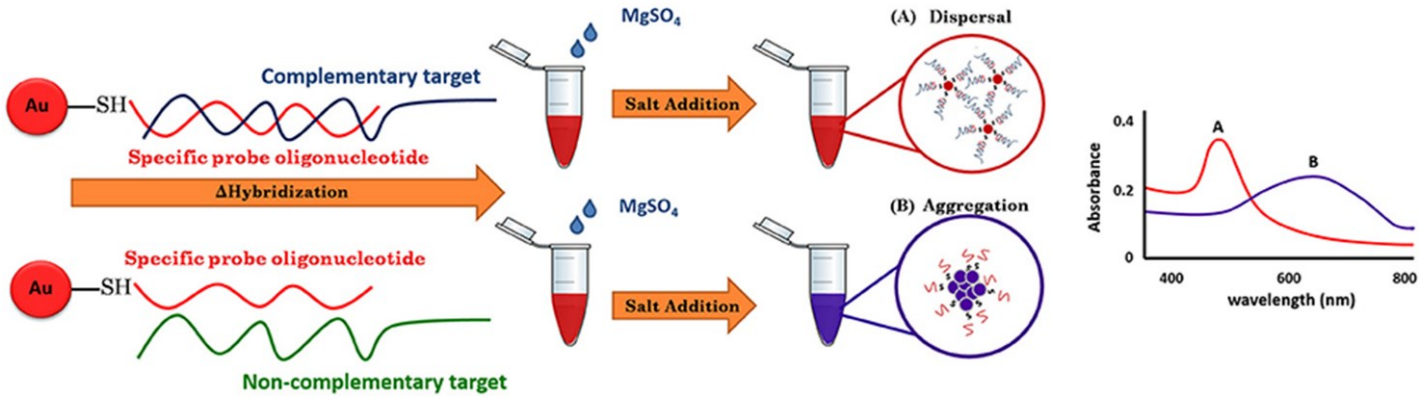
Au
SH
Complementary target
Specific probe oligonucleotide
ΔHybridization
Specific probe oligonucleotide
Au
SH
Non-complementary target
MgSO4
Salt Addition
(A) Dispersal
MgSO4
Salt Addition
(B) Aggregation
Absorbance
0.4
0.2
0
A
B
400
600
800
wavelength (nm)

B

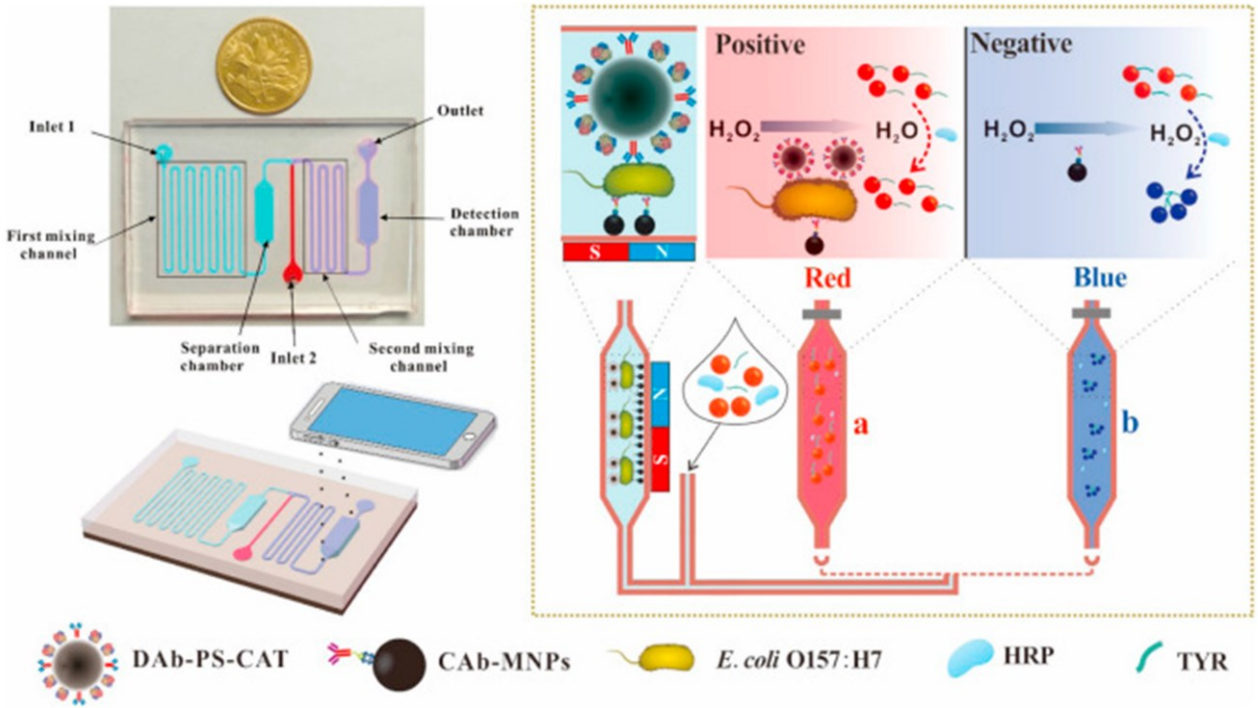
Inlet 1
Outlet
First mixing channel
Detection chamber
Separation chamber
Inlet 2
Second mixing channel
Positive
Negative
H2O2
H2O
H2O2
H2O2
S
N
Red
Blue
a
b
DAb-PS-CAT
CAb-MNPs
E. coli O157:H7
HRP
TYR